To the Graduate Council:

I am submitting herewith a thesis written by Mary Lynn Dobson entitled "Petrography, Chemistry, and Origin of Fe-Ti Oxides in the Concord Gabbro-Syenite, North Carolina." I have examined the final copy of this thesis for form and content and recommend that it be accepted in partial fulfillment of the requirements for the degree of Master of Science, with a major in Geology.

Kula C. Misra

Kula C. Misra, Major Professor

We have read this thesis and recommend its acceptance:

Lawrence A. Taylor

Harry G. McSween

Accepted for the Council:

C W Minkel

Vice Provost
and Dean of The Graduate School

STATEMENT OF PERMISSION TO USE

In presenting this thesis in partial fulfillment of the requirements for a Master of Science degree at The University of Tennessee, Knoxville, I agree that the Library shall make it available to borrowers under rules of the Library. Brief quotations from this thesis are allowable without special permission, provided that accurate acknowledgment of source is made.

Permission for extensive quotation from or reproduction of this thesis may be granted by my major professor, or in his absence, by the Head of Interlibrary Services when, in the opinion of either, the proposed use of the material is for scholarly purposes. Any copying or use of the material in this thesis for financial gain shall not be allowed without my written permission.

Signature Mary Lynn Dobson

Date August 17, 1987

PETROGRAPHY, CHEMISTRY, AND ORIGIN OF FE-TI OXIDES IN THE CONCORD GABBRO-SYENITE, NORTH CAROLINA

A Thesis

Presented for the

Master of Science

Degree

The University of Tennessee, Knoxville

Mary Lynn Dobson

December 1987

ACKNOWLEDGMENTS

Special thanks go to Kula Misra for his patient supervision during the preparation of this thesis. I am also grateful to my committee members, Hap McSween and Larry Taylor, who provided both encouragement and criticism when and where I needed them most. I am indebted to my friends both in and out of the department, my family, and especially Bob Eklund, for their support, consideration, and confidence in me during the course of this research.

ABSTRACT

The Concord intrusive complex consists of a differentiated gabbroic stock, partially encircled by a horseshoe-shaped syenite ring dike that may be related to the gabbro through closed-system fractional crystallization. The oxide phases comprise from two to twelve modal percent, and occur in several textural varieties: (a) discrete magnetite grains with ilmenite granules, laths, and lamellae, as well as pleonaste blebs and needles; (b) discrete ilmenite grains sometimes containing hematite; (c) symplectic intergrowths of oxide vermicules in orthopyroxene matrix; and (d) rods and platelets in clinopyroxene and orthopyroxene. Early forming cumulus magnetite with olivine and abundance of hydrous minerals reflect crystallization conditions characterized by high water activity and elevated fO_2. The present textures and compositions of the oxide minerals show evidence of substantial subsolidus reequilibration. Nevertheless, evidence for magmatic differentation is preserved in the compositions of the oxide minerals. Steady increases in the hematite content of ilmenite suggest that relative fO_2 increased with differentiation. Variations of the minor elements in both magnetite and ilmenite reflect a similar differentiation trend. The variation of the major elements were controlled by elevated fO_2 and an increasing degree of exsolution. Ilmenite was oxy-exsolved from magnetite, forming external and internal granules, laths, and lamellae. Each stage of ilmenite exsolution caused supersaturation of Al_2O_3 in the magnetite host, resulting in an imposed exsolution of pleonaste in the magnetite to produce ilmenite-pleonaste intergrowths. Hematite textures in

ilmenite reflect increasing hematite content and the process of exsolution. Below 15 mol % hematite, ilmenite exsolved a single set of hematite lenses of uniform size; above 15 mol % hematite, exsolution in ilmenite gave rise to two sets of hematite lenses (synneusis texture). Symplectic intergrowths of orthopyroxene and iron-titanium oxides usually occur at borders of olivine grains adjacent to discrete oxide grains. Clear replacement textures, such as cuspate boundaries, optically continuous islands of olivine, and pseudomorphs, indicate that olivine was replaced by symplectic intergrowths. The oxide phases of the symplectite vary as the phases present in the associated oxide grain. Textural evidence and phase chemistry indicate that the mechanism of formation of the symplectic intergrowth involved more than the simple oxidation of olivine. Late magmatic melt and discrete oxide grains may also have taken part in the symplectic formation.

TABLE OF CONTENTS

CHAPTER		PAGE
I.	INTRODUCTION	1
II.	PREVIOUS WORK	3
III.	OXIDE MINERAL PETROGRAPHY	7
	Modal and Textural Variations	7
	Discrete Oxide Grains	11
IV.	OXIDE MINERAL CHEMISTRY	37
	Phase Compositions	37
	Zoning	44
	Primary Igneous Trends Preserved in Oxide Compositions	47
V.	PETROGENESIS OF OXIDE MINERALS	53
	Magnetite	53
	Ilmenite Exsolution	55
	Pleonaste Exsolution	56
	Hematite Exsolution	59
	Symplectic Intergrowths	60
VI.	CONCLUSIONS	67
REFERENCES		69
VITA		75

LIST OF TABLES

TABLE		PAGE
1.	Modal Analyses (Volume Percent) of Samples from the Concord Intrusive Complex	9
2.	Point Counts of Ten Symplectic Intergrowths to Determine Volume Percent of Magnetite and Orthopyroxene	33
3.	Representative Microprobe Analyses of Associated Oxide Phases in Discrete Magnetite Grains	39
4.	Partitioning Coefficients Calculated from Microprobe Analyses Given in Appropriate Tables	40
5.	Representative Microprobe Analyses of Ilmenite and Associated Hematite Lenses	42
6.	Microprobe Analyses of Oxide Vermicules in Symplectites and Associated Discrete Oxide Grains	43
7.	Representative Microprobe Analyses of Zonation in Ilmenite Next to Magnetite	46
8.	Representative Microprobe Analyses of Magnetite Vermicules and Orthopyroxene in Symplectic Intergrowths and Associated Olivine Grains	62
9.	Calculation by Weight of Gains and Losses of MgO, FeO, and SiO_2 (with Excess Oxygen) in an Idealized Reaction of Olivine Forming a Magnetite-Orthopyroxene Symplectic Intergrowth	63

LIST OF FIGURES

FIGURE		PAGE
1.	Geologic Map of the Concord Intrusive Complex	5
2.	Molar Compositions of Ferromagnesian Silicates in the Concord Gabbro and Syenite	6
3.	Correlation of Textural Varieties of Oxide Phases with Rock Types of the Concord Complex	8
4.	Correlation of Modal Variation of Oxide Textural Types with the Differentiation Sequence for the Concord Complex as Proposed by Olsen et al. (1983)	10
5.	Textures of Discrete Magnetite Grains in Reflected Light	12
6.	Ilmenite-Hematite Exsolution Textures in Reflected Light	17
7.	Occurrence of Symplectic Intergrowths	21
8.	Photomicrograph and Drawing of Serpentinized Olivine with a Cuspateboundary, Partially Replaced by Symplectic Intergrowth	23
9.	Photomicrograph and Drawing of Possible Pseudomorph of Symplectic Intergrowth After Olivine	25
10.	Photomicrograph and Drawing of Olivine Grain Surrounded by Poikilitic Hornblende and Partially Replaced by Symplectic Intergrowth of Orthopyroxene, Magnetite, and Ilmenite in the Area Adjacent to a Discrete Oxide Grain	27
11.	Oxide Exsolution in Pyroxenes	34
12.	Phase Chemistry of Coexisting Oxide Minerals in the Four Rock Types of the Concord Igneous Complex	38
13.	Variation Diagrams of the Major Elements in Magnetite and Ilmenite with Different Rock Types	49
14.	Variation Diagrams of the Minor Elements in Magnetite and Ilmenite with Different Rock Types	50
15.	Schematic Diagram of the Crystallization History in the Concord Complex	54

CHAPTER I

INTRODUCTION

A linear trend of postmetamorphic gabbroic plutons extends for at least 500 km in the southern Appalachian Piedmont. Previous studies of these gabbroic complexes have concentrated on the mineral chemistry, textures, and occurrences of the silicate minerals in an effort to provide information on their genesis. Iron-titanium oxide minerals comprise a small but significantpart of these intrusive complexes. Their occurrences in several textures and associations suggest various methods of formation and a complex subsolidus history. Studies of Fe-Ti oxides in rocks at other locations have provided information on crystallization conditions, magmatic evolution, and subsolidus reactions within the host rock (Vincent and Phillips, 1954; Duchesne, 1972; Czamanske and Mihalik, 1972; Mathison, 1975; Himmelberg and Ford, 1977; Thy, 1982; and von Gruenewaldt et al., 1985). The purpose of this thesis is to conduct a systematic study of the Fe-Ti oxides found in one of the southern Appalachain postmetamorphic intrusive complexes.

The Concord intrusive complex of Carbarus County, North Carolina is an excellent choice for this study as it provides a chance to study the oxide minerals of both a gabbroic body and its associated syenite ring dike. A previous study of this complex suggested a petrogenetic relationship for gabbro and syenite through closed-system fractionation (Olsen et al., 1983). Detailed information on the textures, compositions, and subsolidus reactions of the oxide minerals may provide

a better understanding of the crystallization conditions and subsolidus history of the host rock.

CHAPTER II

PREVIOUS WORK

The Concord intrusive complex is located in the Charlotte slate belt of the Piedmont. The Piedmont differs in metamorphic, deformational and igneous history from its adjacent provinces, and may have been accreted onto the continent (Williams and Hatcher, 1982). The gabbroic complexes in the Piedmont have been interpreted as part of the plutonic core of this Paleozoic arc system emplaced at a convergent plate boundary (McSween et al., 1984). Petrological studies of several of the Charlotte belt gabbros have been published (Hermes, 1968, 1970; Medlin et al., 1972; McSween and Nystrom, 1979; Olsen et al., 1983). Previous studies of the Concord intrusive complex include Watson and Laney (1906), Butler and Ragland (1969), Cabaup (1969), Fullagar (1971), Olsen et al. (1983), and McSween (1986).

A detailed description of the geological setting and major features of the Concord intrusive complex is included in Olsen et al. (1983). Only a brief summary of those features is offered here. The complex consists of an oval-shaped gabbroic body partially encircled by a horseshoe-shaped syenite ring dike. The gabbro, roughly 10.8 km in diameter north to south and 6.7 km east to west, was emplaced 407 $\pm$ 36 m.y. ago. Geophysical modelling suggests that it extends to a depth of roughly 6 km. The syenite dike ranges in thickness from 0.5 km to 2.5 km at the surface and was emplaced 404 $\pm$ 21 m.y. ago. The west limb of the syenite dike dips steeply outward at about 78° while the east limb

appears to be vertical. Both the gabbro and syenite are cut by later pegmatite and diabase dikes. As shown in Figure 1, the complex is intrusive into dioritic and mafic rocks that have been regionally metamorphosed to amphibolite facies. Gneissic, granitic, and granodioritic rocks abut the syenite on both the east and west sides.

The Concord gabbro is a differentiated pluton, described by Olsen et al. (1983) as containing "medium-grained meso- and orthocumulates consisting primarily of plagioclase, olivine, clinopyroxene, orthopyroxene, and amphibole, with lesser amounts of biotite, oxide and sulfide minerals, apatite, and alteration products." The classification of rock types set forth in Olsen et al. (1983) is based on assemblages of cumulus minerals present in the gabbro and reflects texturally the following fractionation trend: olivine-plagioclase cumulate (OPC), olivine-clinopyroxene-plagioclase cumulate (OCPC), and clinopyroxene-plagioclase cumulate (CPC). The syenite (CS) is described by Olsen et al. (1983) as "a coarse-grained, seriate porphyry containing large phenocrysts of perthite and antiperthite in a groundmass of perthite, plagioclase, microcline, clinopyroxene, biotite, amphibole, quartz, oxide and sulfide minerals, zircon, apatite and monazite." In the sequence OPC, OCPC, CPC, and CS, fractionation is chemically manifested by the iron enrichment trends of the ferromagnesian minerals (Figure 2) and the sodium enrichment trends of the plagioclase cores (Olsen et al., 1983).

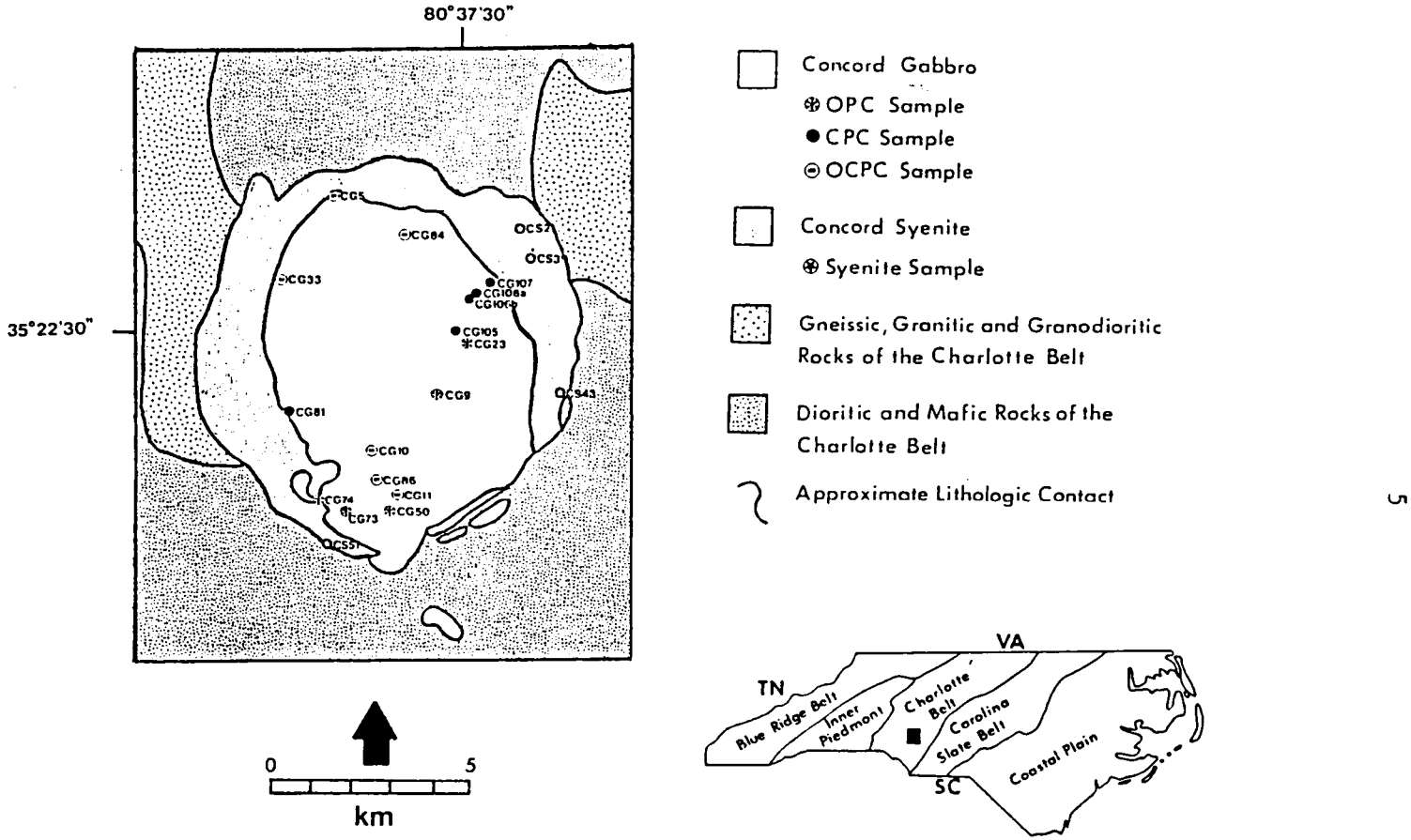

Figure 1. Geologic map of the Concord intrusive complex. Locations of gabbro (CG) and syenite (CS) samples given. The inset map shows the location of the complex within the Charlotte belt in the North Carolina Piedmont. After Olsen (1982).

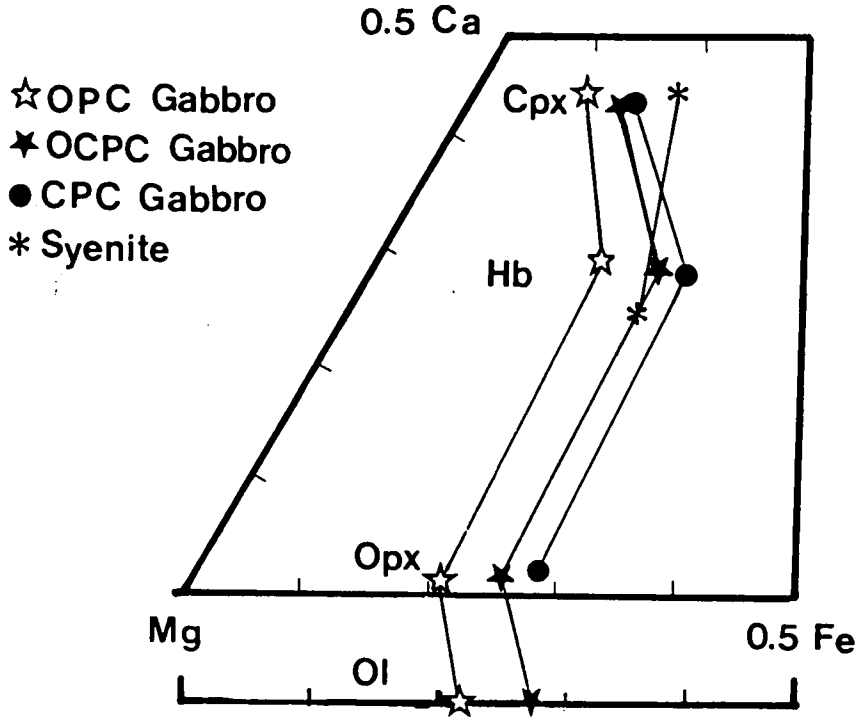

Figure 2. Molar compositions of ferromagnesian silicates in the Concord gabbro and syenite. Clinopyroxene (Cpx), hornblende (Hbl), orthopyroxene (Opx), and olivine (Olv), coexisting in the same sample are joined by tie-lines. All of these phases are homogeneous. Modified from Olsen et al.(1983).

CHAPTER III

OXIDE MINERAL PETROGRAPHY

Modal and Textural Variations

Oxide minerals are ubiquitous in the Concord intrusive complex, and occur in several textural varieties: (a) discrete magnetite grains with ilmenite granules, laths, and lamellae, as well as pleonaste blebs and needles; (b) discrete ilmenite grains, some containing hematite; (c) symplectic intergrowthwith orthopyroxene; and (d) rods and platelets in clinopyroxene and orthopyroxene. Figure 3 relates the mineral textures of the oxides to the rock types in which they are found. Modal analyses from two polished thin sections of each rock type are presented on Table 1. Total oxide mineral abundance is highest in the earliest formed OPC rocks and decreases slightly in the OCPC and CPC samples. The oxide mineral content in the syenite drops sharply, from an average of about 5.4% in the CPC to about 2.2% in the syenite. A parallel drop of modal abundances is found in the mafic silicate minerals of the syenite (Olsen, 1982). Figure 4 illustrates modal variations of the dominant oxide textures with respect to rock type and increasing differentiation. Magnetite volume percent decreases from the OPC to the OCPC, but rises sharply in the CPC samples which do not contain olivine. The lowest concentration of magnetite is found in the syenite. Abundance of discrete ilmenite is lowest in the earliest-forming rock type (OPC); it increases steadily with fractionation, and in the syenite represents over half of all oxides present. Increasing concentrations

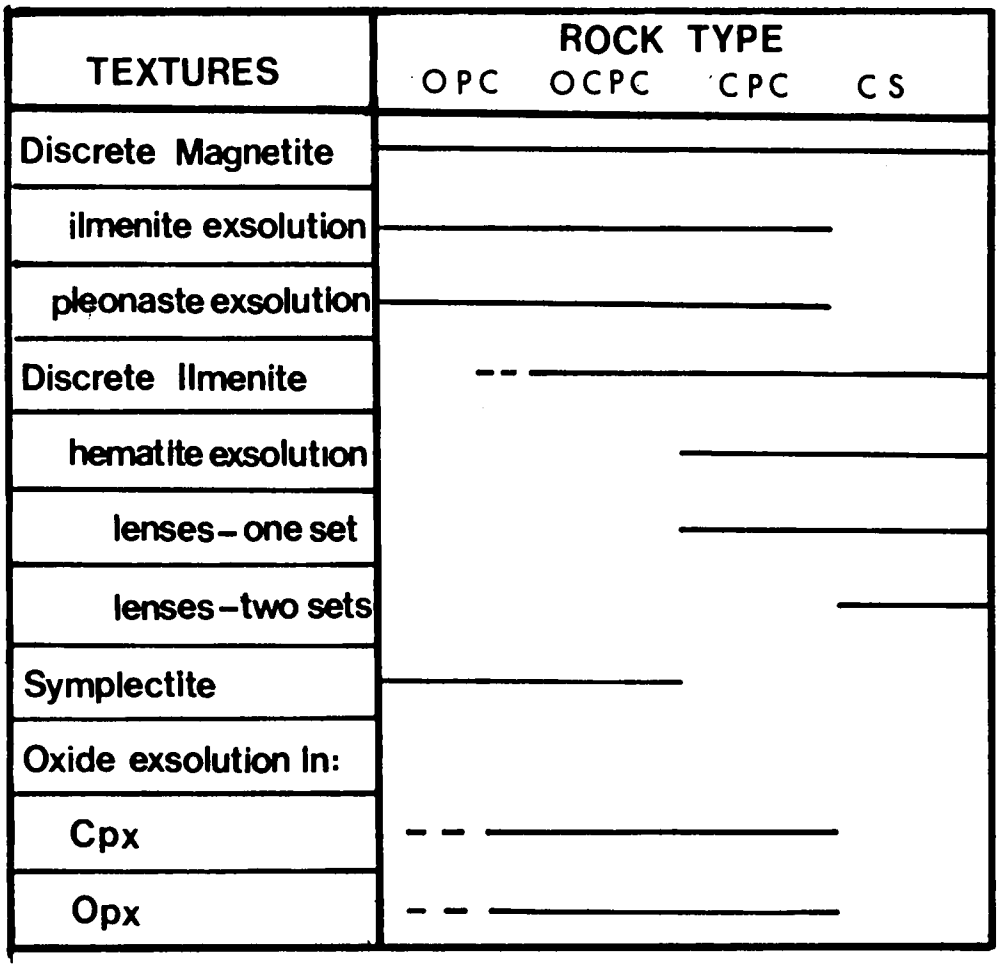

Figure 3. Correlation of textural varieties of oxide phases with rock types of the Concord complex.

Table 1. Modal Analyses (Volume Percent) of Samples from the Concord Intrusive Complex. Number of Points Counted Per Sample = 2000. 30% of Total Symplectic Counts Are Counted with Oxide Minerals. Mag = Magnetite, Ilm = Ilmenite, Gran = Granule, Sym = Symplectite.

Rock Type	Sample No.	Silicate	Sulfide	Oxides				
				Discrete Mag Grain		Discrete		
				Mag	Ilm Gran	Ilm	Sym	Total
Gabbro (OPC)	Cg-9	92.65	0.90	4.30	0.90	0.05	1.15	5.60
	Cg-73	93.45	0.30	4.25	0.85	0.05	1.10	5.48
Gabbro (OCPC)	Cg-11	94.15	0.35	2.60	0.70	0.10	2.10	4.03
	Cg-58	95.40	0.30	2.15	0.70	0.30	1.15	3.50
Gabbro (CPC)	Cg-106B	94.15	0.45	4.05	0.60	0.75	0	5.40
	Cg-81	94.20	0.30	3.60	0.70	1.20	0	5.50
Syenite (CS)	CS-12	97.40	0.10	0.90	0.25	1.35	0	2.50
	CS-43	98.00	0	0.65	0.15	1.20	0	2.00

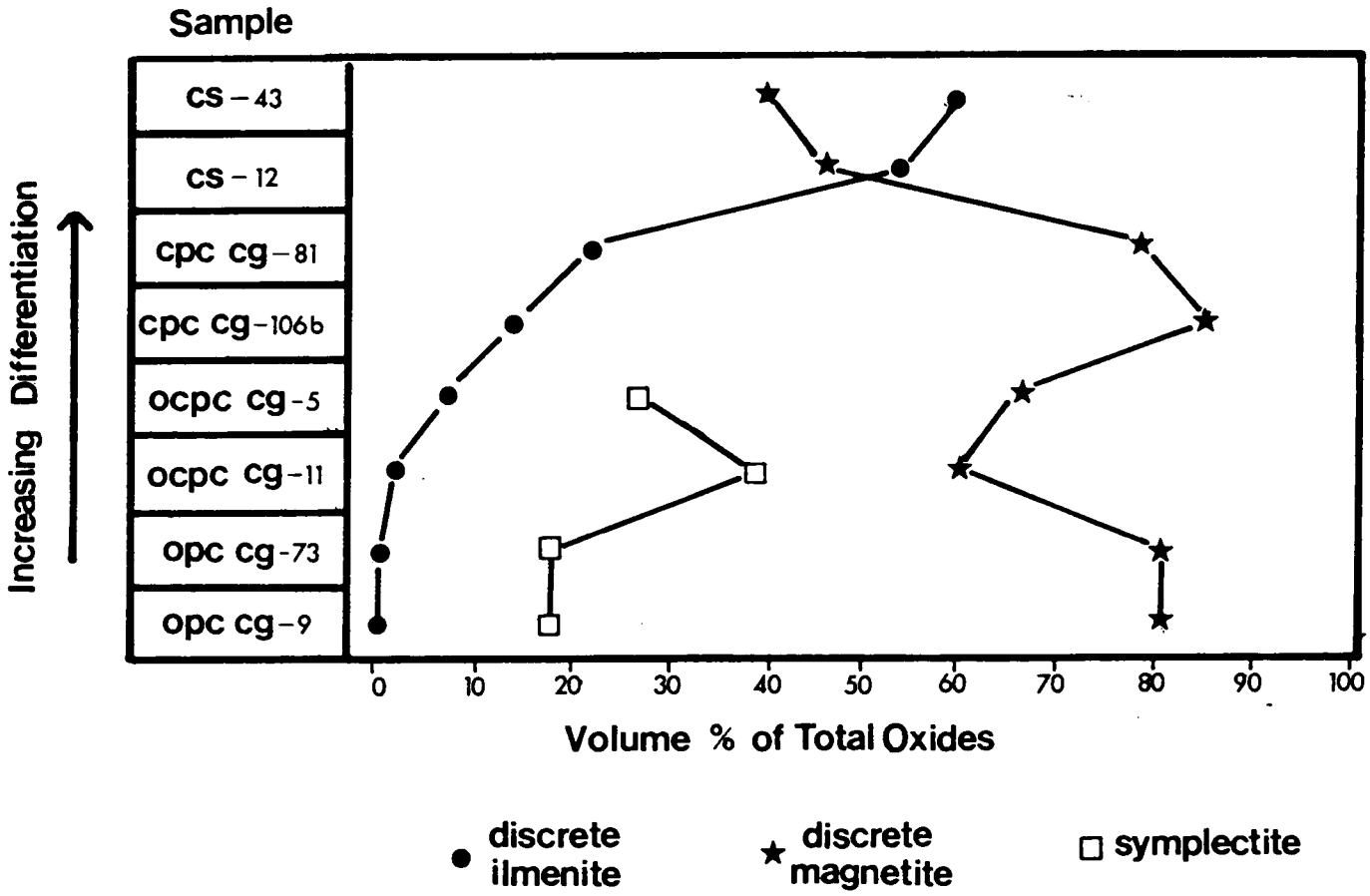

Figure 4. Correlation of modal variation of oxide textural types with the differentiation sequence for the Concord complex as proposed by Olsen et al. (1983).

(i.e., activity) of Ti in the residual melt may have resulted in increasing crystallization of discrete interstitial ilmenite grains (Elsdon, 1972). The symplectic intergrowths occur only in the rocks containing olivine. The increase in volume percent of symplectite from OPC to OCPC may reflect the increasing degree of disequilibrium between olivine and melt with progressive fractionation.

Discrete Oxide Grains

Magnetite. Magnetite occurs as subhedral to anhedral isolated discrete grains. It is not homogeneous, but contains three forms of ilmenite intergrowths: trellis lamellae, sandwich laths, and granules. The magnetite of the gabbroic samples also contain intergrowths of pleonaste.

Small euhedral to subhedral cumulus magnetite grains (Fig. 5A) are found in all rock samples of the gabbro, occurring in the greatest abundance in OPC, the earliest forming rock type, but are absent in the syenite. These cumulus grains are smaller than the interstitial oxide grains, averaging 0.2 mm in diameter. They are enclosed by cumulus silicates as well as larger, interstitial silicate grains. The uniform shape and size of these grains, together with their occurrence within other cumulus and intercumulus silicates, indicate that these are early formed cumulus grains.

Consistently larger than the cumulus magnetite, the anhedral interstitial oxide grains average roughly 1.0 mm in diameter. The

Figure 5. Textures of discrete magnetite grains in reflected light. Bar scales represent 0.25 mm, except B and F. MAG = Magnetite. ILM = Ilmenite. PLEO = Pleonaste.

A. Subhedral cumulus magnetite grain. Sample Cg-9.

B. Anhedral, interstitial magnetite grain. Bar scale represents 1.5 mm. Sample Cg-11.

C. Ilmenite laths grading into internal granule. Pleonaste occurs as blebs within ilmenite laths, and at magnetite-silicate grain boundry. Sample Cg-9.

D. Trellis texture of ilmenite lamellae in magnetite, enhanced by etching with HCl. Sample Cg-74.

E. Ilmenite laths containing pleonaste blebs. Pleonaste also occurs as dissemenated needles. Sample Cg-33.

F. Pleonaste needles crosscutting and at times offsetting ilmenite lamellae (arrows). Bar scale represents 0.05 mm. Sample Cg-74.

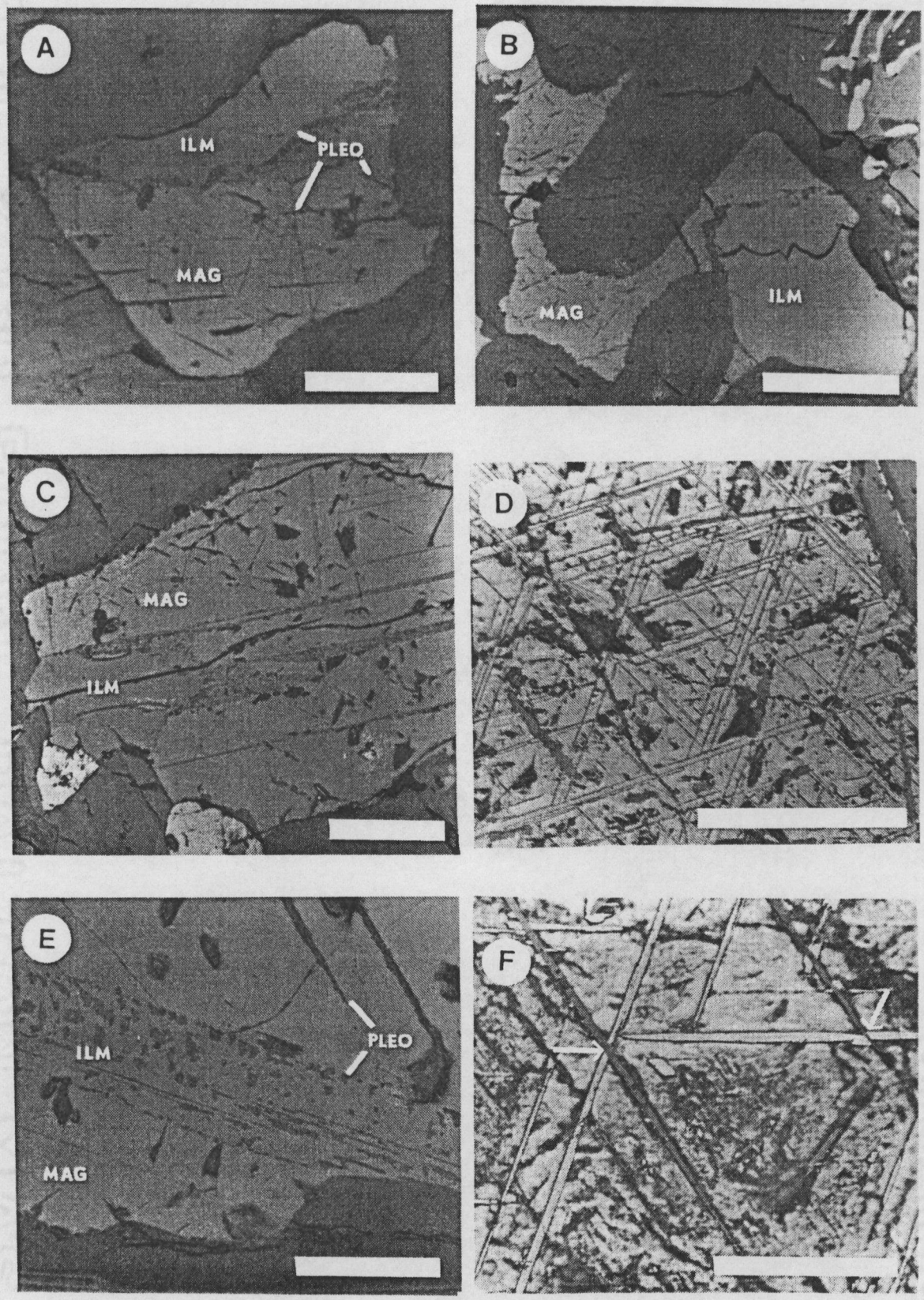

Figure 5 (continued)

interstitial grain may partially surround a cumulus phase (Fig. 5B), indicating that it formed later than the cumulus minerals.

Ilmenite intergrowths in magnetite occur as trellis, lath, and granule internal exsolution textures, as well as an external ilmenite granule exsolution texture (classification of ilmenite textures in magnetite from Buddington and Lindsley, 1964). "Exsolution" is used in this paper to refer to both true (isochemical) exsolution and oxidation-exsolution as defined by Buddington and Lindsley (1964). The large magnetite granule with internal ilmenite exsolution may share one or more grain boundaries with the companion external ilmenite granule. The boundaries between the two granules are straight, sealed, and clear of silicate material. Pleonaste blebs may occur at the magnetite border or inside the ilmenite granule or lath. Gradation between internal and external ilmenite granules (Fig. 5C) occurs in all gabbroic samples.

In the syenite, the magnetite appears homogeneous, and all oxide grains have anhedral boundaries. Although isolated single grains exist, the oxides occur most commonly as elongate clusters of randomly oriented grains. These clusters appear to have incidental numbers of both magnetite and ilmenite grains, some clusters consisting of all ilmenite grains, some all magnetite, while most are a mixture of the two. Pleonaste does not occur within the magnetite grains. The occurrence of oxide grains in clusters, the absence of pleonaste at the common boundary between magnetite and ilmenite, and the absence of compositional difference between discrete ilmenite and ilmenite granules

make it difficult to determine if any ilmenite granules exist in the syenite.

In the gabbro, magnetite grains are not homogeneous, but are always host to fine ilmenite lamellae presumably oriented along the {111} planes of magnetite. Because these lamellae usually occur in three directions in the magnetite host, they are aptly described as trellis texture (Fig. 5D). All lamellae parallel to one trellis direction show simultaneous extinction and equal width throughout their length. Many magnetite grains also host one or more thick ilmenite sandwich laths. These laths, oriented along a preferred set of the {111} planes of magnetite, occur both within the core of the magnetite grains and along the grain boundaries (Fig. 5E).

Pleonaste is found in all observed magnetite samples in the gabbro, but not in any of the syenite samples. Pleonaste occurs within magnetite in two textures: as small, rounded blebs, and as tiny needles, presumably oriented along the {100} planes of magnetite. The pleonaste needles occur within the magnetite and also within the ilmenite lamellae and sandwich laths of the magnetite host. The blebs, some as large as 0.013 mm but mostly smaller, occur around the border of the magnetite grains at both the ilmenite and silicate shared grain boundaries. Commonly the pleonaste blebs are found inside ilmenite laths or granules near the shared magnetite boundary (Figs. 5A, B, and C).

No ulvöspinel exsolution was visible in magnetite in any of the polished thin sections. The method of enhancing ulvöspinel and ilmenite intergrowth texture in magnetite grains by etching with HCl, as

described by Duchesne (1970), was tried on polished thin sections of OPC, CPC, and syenite rock types. The etching was successful in enhancing the trellis texture of the ilmenite lamellae, but the "cloth texture" typical of ulvöspinel intergrowth with magnetite was not found in any of the sample tested.

Ilmenite-Hematite. Ilmenite is present in the Concord rock suite as internal and external intergrowths associated with magnetite, which are interpreted as exsolutions, as well as discrete isolated grains that appear to have crystallized directly from the melt. The discrete ilmenite grains are similar to the anhedral magnetite grains in both shape and size. Ilmenite discrete grains and granules have similar exsolution textures and compositions within each rock type. In the syenite, ilmenite is clustered with magnetite and mafic minerals.

Ilmenite appears texturally homogeneous in the OPC and OCPC rock types, but contains hematite lenses of varing sizes. These are oriented parallel to the {0001} direction of ilmenite in the CPC and CS rock samples. In the CPC rock samples, hematite occurs as small elongate exsolution lenses evenly distributed throughout the ilmenite. The lenses are consistent in size within each grain, but vary in size from one grain to another within a one inch diameter polished thin section (Fig. 6A). In the syenite, many ilmenite grains contain two sets of hematite lenses, forming a synneusis texture. This texture is described by Haggerty (1976) as "finer lenses of the solute (exsolving phase) distributed between thicker lenses in the solvent (host-dissolving medium)." The second set of exsolved lenses is largest midway between

Figure 6. Ilmenite-hematite exsolution textures in reflected light. Bar scales represent 0.1 mm. ILM = Ilmenite. HEM = Hematite. SUL = Sulfide. MAG = Magnetite.

A. One set of hematite lenses in ilmenite. Zoning of hematite lenses as magnetite grain is approached. Sample Cs-12.

B. Two sets of hematite lenses (synneusis texture) in ilmenite. Sample Cs-43.

C. Zoning of hematite lenses in ilmenite as sulfide grain is approached. Sample Cs-21.

D. Zoning of hematite lenses in ilmenite as magnetite and sulfide grains are approached. Sample Cg-106A.

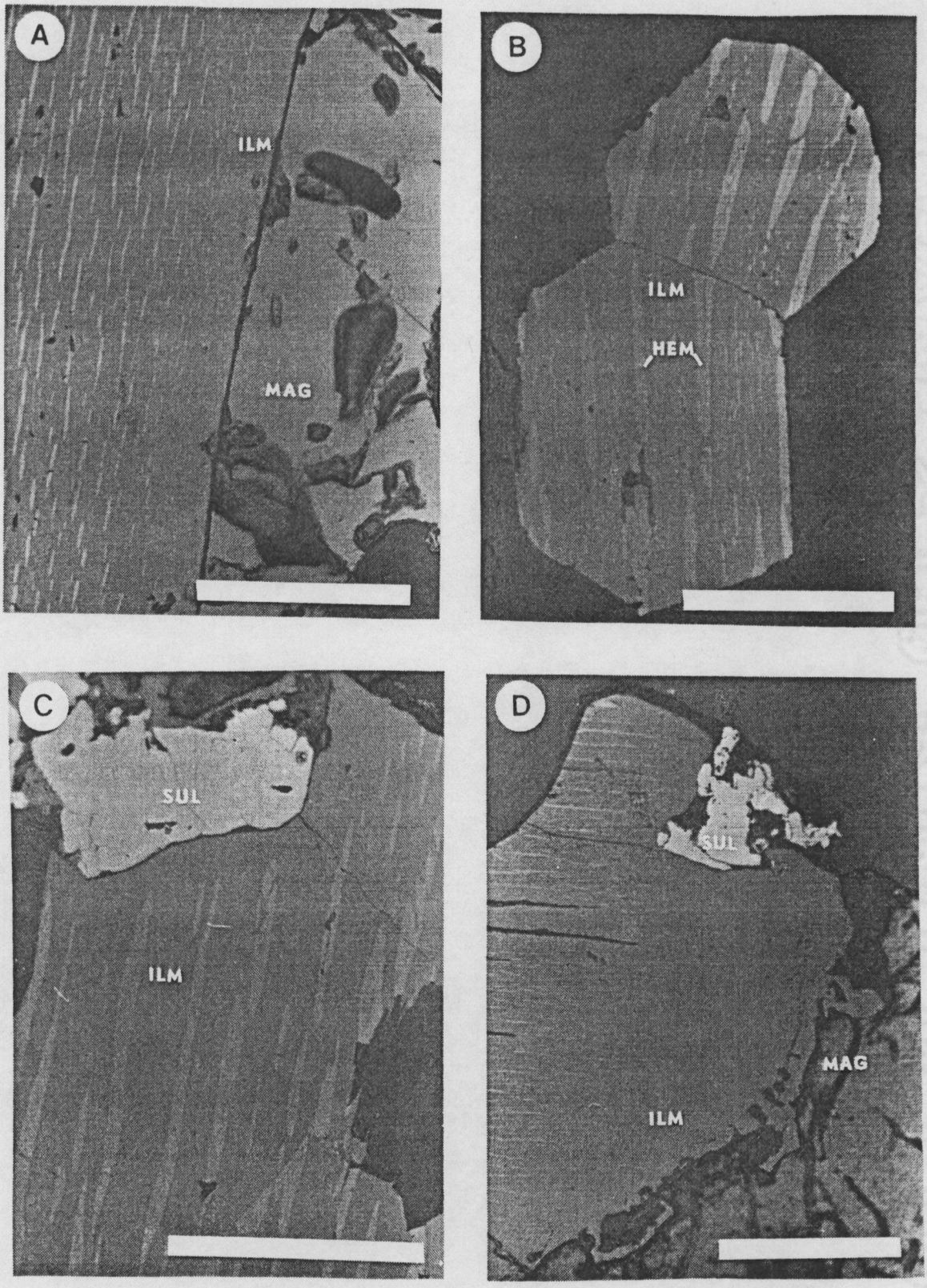

Figure 6 (continued)

two coarse first generation lenses, and decrease in size as the larger lenses are approached. Often the secondary lenses are only visible in the central areas between the coarser exsolution bodies. Some of the larger hematite lenses in the syenite samples contain tiny ilmenite exsolution bodies parallel to the {0001} direction of both the large hematite lenses and the ilmenite host grain (Fig. 6B). These ilmenite lenses occur only when there are also secondary hematite exsolution bodies, but the second generation hematite is sometimes visible in grains that do not show ilmenite exsolution in the coarse hematite lenses.

Zoning occurs when ilmenite grains with hematite exsolution share a common boundary with a magnetite or a sulfide grain. The visible hematite exsolution decreases as the magnetite or sulfide border is approached, leaving the ilmenite near the shared border visibly free of hematite exsolution (Figs. 6A,C,and D). This ilmenite zoning occurs only at the magnetite or sulfide contacts, and not at silicate contacts, or at contacts between two ilmenite grains.

Symplectic intergrowths. Various kinds of symplectic intergrowths between oxides and orthopyroxene have been described in the literature. These occur either as coronas around olivine grains (Esbensen, 1978; van Lamoen, 1979; Garrison and Taylor, 1981; Otten, 1983) or as reaction replacements of an area of the olivine grains (Ambler and Ashley, 1977; McSween and Nystrom, 1979). Haselton and Nash (1975) and Daval (1987) have described similar intergrowths without olivine association. Most

authors attribute the sympletic intergrowths to a breakdown of cumulus olivine grains caused by one of the following mechanisms:

1. subsolidus oxidation (Muir et al., 1957; Haggerty and Baker, 1967; Goode, 1974; Esbensen, 1978; van Lamoen, 1979; Otten, 1983);
2. back-reaction with residual liquid to form orthopyroxene and magnetite (Ambler and Ashley, 1977; McSween, 1980); or
3. resorption by residual liquid with simultaneous precipitation of orthopyroxene and magnetite (Garrison and Taylor, 1981).

Van Lamoen (1979) and Otten (1983) noticed that the symplectic intergrowths usually occur adjacent to discrete oxide grains, but did not attribute the formation of symplectite to a reaction between oxide and olivine.

Symplectic intergrowths of oxide and orthopyroxene (Figs. 7, 8, 9, and 10) are found in all but one of the olivine-bearing rocks (OPC and OCPC) studied. They do not occur in any rock sample in which olivine is absent. Sample Cg-84 (OCPC) is the only olivine bearing rock that did not contain symplectic intergrowths. It is very fine-grained, suggesting a faster rate of cooling that may have inhibited diffusion. The absence of oxide exsolution lamellae in pyroxene in this sample supports this possibility.

Symplectic intergrowths vary in size from tiny areas to relatively large blebs approaching the size of cumulus grains. The intergrowths consist of wormy oxide vermicules, radiating and branching in an orthopyroxene matrix. A small rim of orthopyroxene partially surrounds

Figure 7. Occurrence of symplectic intergrowths. All photomicrographs in reflected light. Bar scales represent 0.25 mm except A). OL = Olivine. OPX = Orthopyroxene. PLEO = Pleonaste. ILM = Ilmenite. MAG = Magnetite.

A. Close-up of symplectic intergrowth. Ilmenite lamellae and pleonaste blebs visible in the magnetite vermicules. Bar scale represents 0.05 mm. Sample Cg-9.

B. Ilmenite discrete grain associated with symplectite that contains mostly ilmenite vermicules. Sample Cg-5.

C. Magnetite of symplectite etched with HCl to enhance ilmenite vermicules. Sample Cg-74.

D. Symplectic intergrowth located between olivine, a discrete oxide grain and poikilitic orthopyroxene. Sample Cg-11.

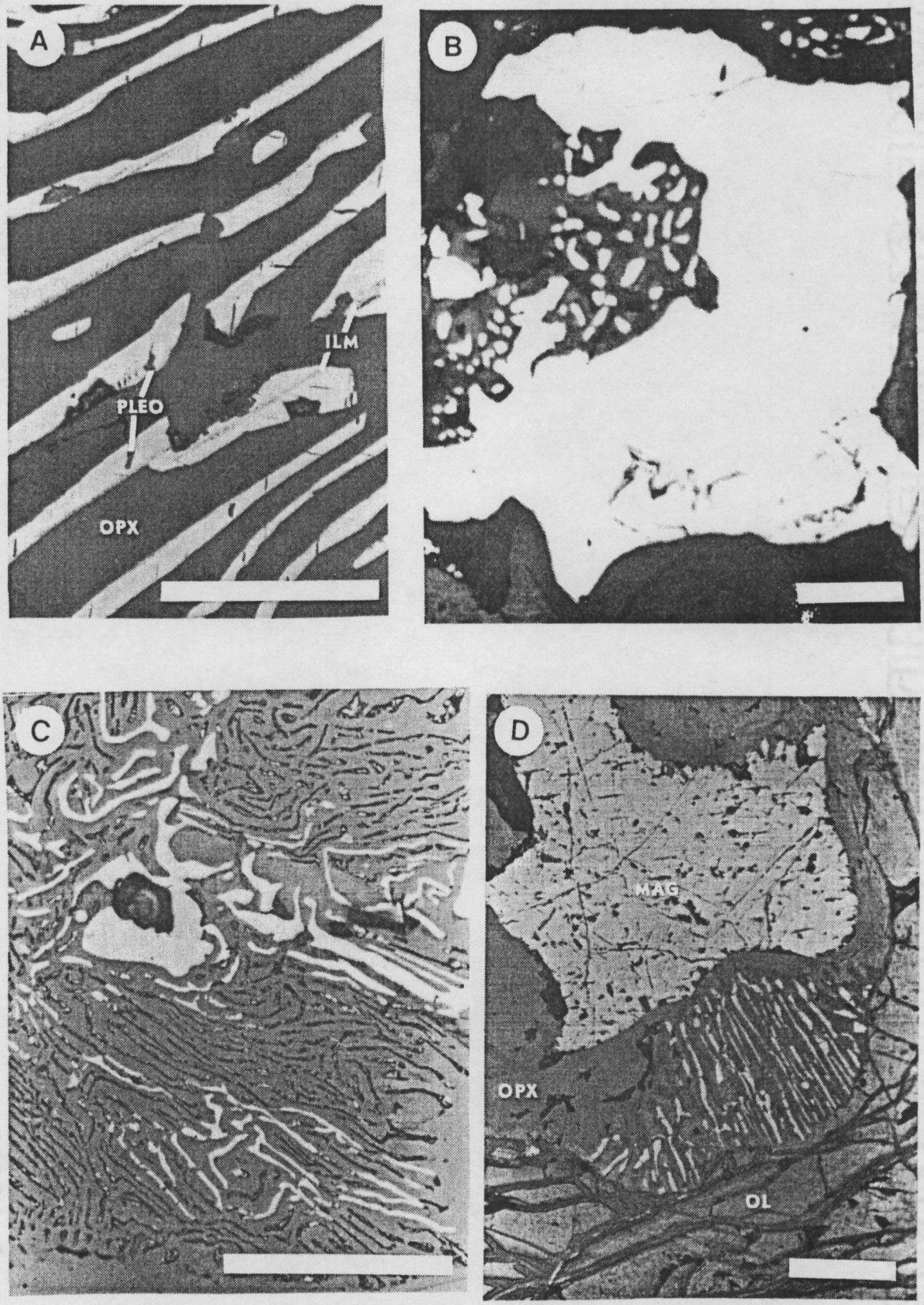

Figure 7 (continued)

Figure 8. Photomicrograph and drawing of serpentinized olivine with a cuspateboundary, partially replaced by symplectic intergrowth. Vermicules increase in size as oxide grain is approached. Photomicrograph in reflected light. Bar scale represents 0.25 mm. Sample Cg-11. Legend to be used for Figures 8, 9, and 10.

LEGEND

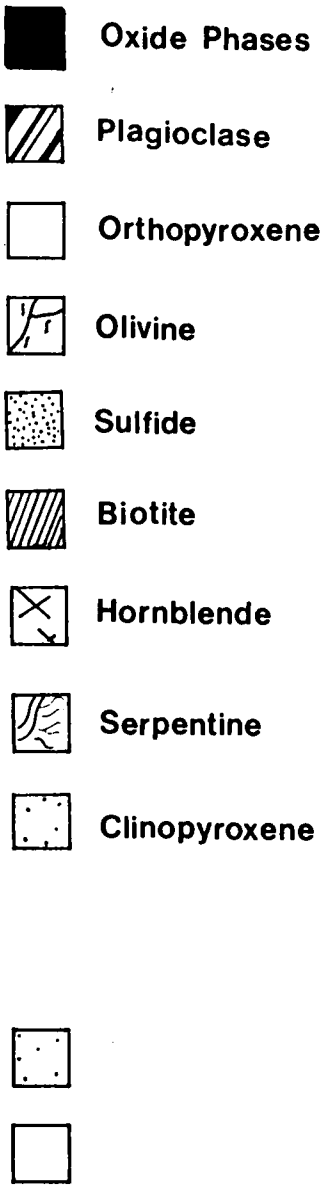

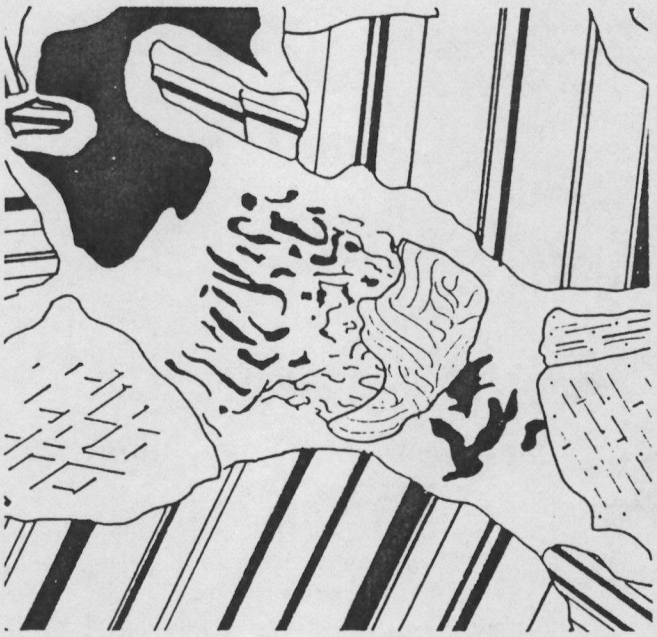

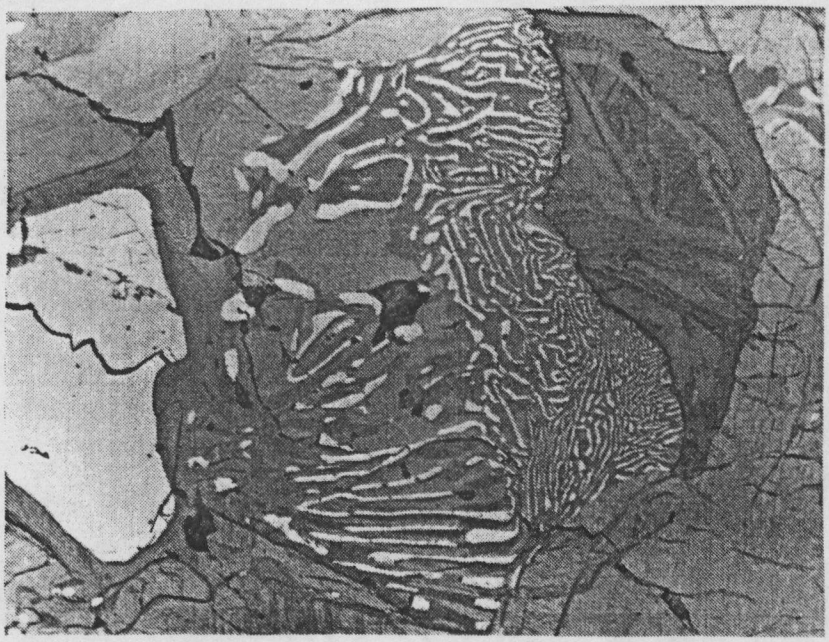

Figure 8 (continued)

Figure 9. Photomicrograph and drawing of possible pseudomorph of symplectic intergrowth after olivine. Photomicrograph in reflected light. Bar scale represents 0.25 mm. Sample Cg-11.

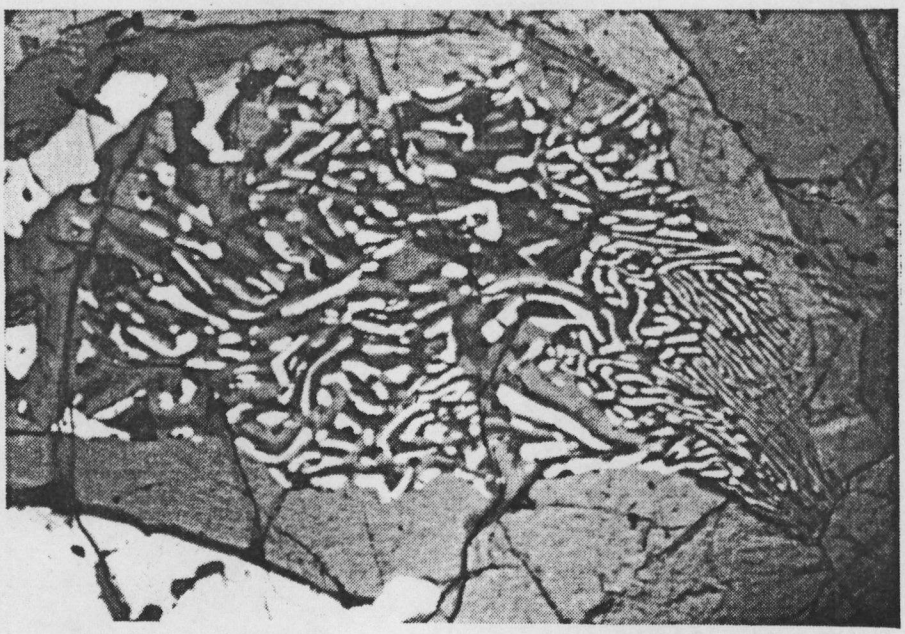

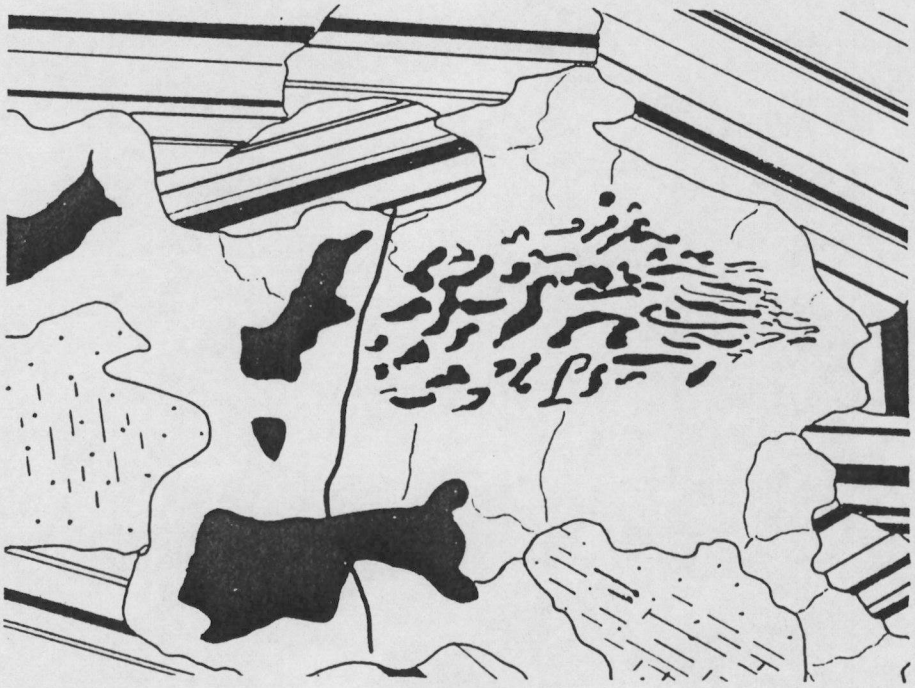

Figure 9 (continued)

Figure 10. Photomicrograph and drawing of olivine grain surrounded by poikilitic hornblende and partially replaced by symplectic intergrowth of orthopyroxene, magnetite, and ilmenite in the area adjacent to a discerete oxide grain. Photomicrograph in both reflected and transmitted light. Bar scale represents 0.5 mm. Sample Cg-73.

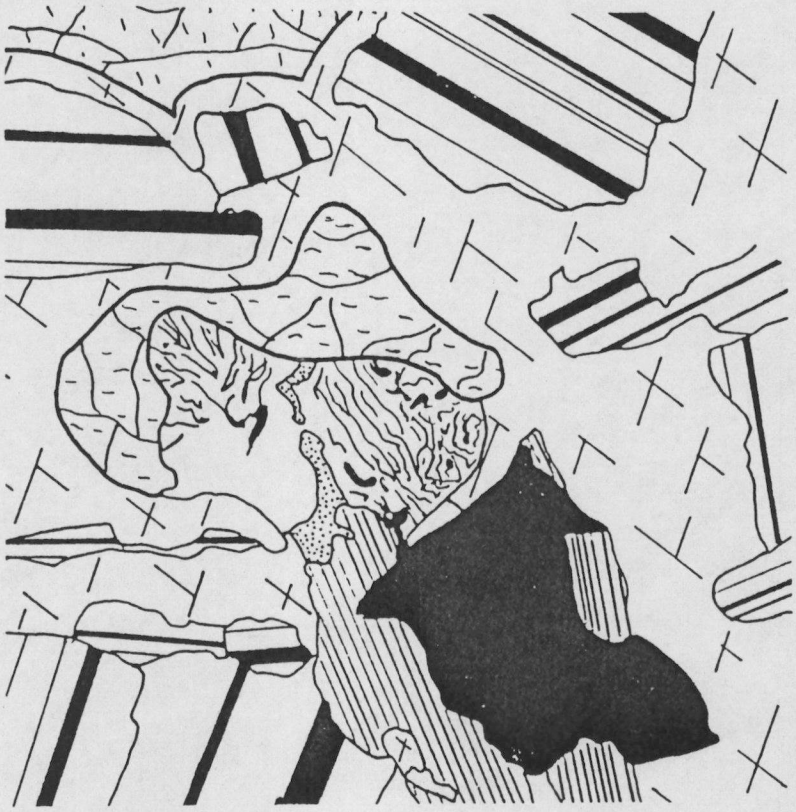



Figure 10 (continued)

the intergrowths. The rim is discontinuous at the olivine symplectite interface (if olivine is present), and in places, discontinuous at the discrete oxide-symplectite interface. The orthopyroxene rim does not exhibit simultaneous extinction, but it is composed of small, almost equant parts that exhibit sequential extinction around the symplectite. In some instances the orthopyroxene in the symplectites has been totally or partially replaced by a brown amphibole resulting in an oxide-amphibole symplectite similar to that mentioned by Ambler and Ashley (1977).

The dominant oxide phase present in the symplectic intergrowths is magnetite. The magnetite vermicules usually contain ilmenite exsolution in the form of laths, needles and blebs. Several samples that contain ilmenite also contain tiny pleonaste exsolution blebs (Fig. 7A). These exsolution textures of ilmenite and pleonaste in the magnetite vermicules are similar to those existing in magnetite grains that have crystallized from the melt. Similar ilmenite intergrowths in magnetite vermicules of symplectites have been found by Ambler and Ashley (1980) and Daval (1987). In symplectites that contain vermicules of both magnetite and ilmenite, the magnetite is usually the dominant mineral, but it is not clear whether the magnetite and ilmenite are separate or are connected elsewhere in the symplectite (Fig. 7C). There are few examples where ilmenite is the only oxide mineral forming the symplectite with orthopyroxene. Where this occurs, ilmenite is also the dominant mineral in the associated discrete oxide grain (Fig. 7B).

The oxide vermicules at times show a variation in size within a given symplectite as has been reported by several authors (Ambler and Ashley, 1977; McSween, 1980; Garrison and Taylor, 1981; Otten, 1983). Out of 80 symplectites studied, 56 showed a decrease in the scale of the wormy intergrowth in a definite direction. The scale of vermicules decreases as the associated olivine is approached and increases as the associated oxide is approached (Figs. 8, and 9). This suggests that the reaction to form the symplectite began near the olivine-oxide grain boundary and extended into the olivine.

In the Concord gabbro, the symplectic intergrowths usually occur at the boundaries of olivine grains adjacent to discrete oxide grains (Figs. 7D, 8, and 10). The area of the symplectite is rounded and does not occur as thin coronas encircling the olivine. The olivine grains show varying degrees of replacement by the symplectites, as well as several distinct replacement textures, such as cuspate boundaries (Fig. 8), optically continuous islands of olivine, and pseudomorphs (Fig. 9). These replacement textures, together with the proximal occurrence of olivine and symplectite, constitute clear evidence that the olivine participated in a reaction to form the symplectic intergrowth. There are many cumulus olivine grains not associated with symplectic intergrowths that are surrounded by late-stage magmatic, poikilitic amphibole or orthopyroxene. Olivine and discrete oxide grains share boundaries without forming symplectite. These textures suggest that olivine, discrete oxide, and melt may be necessary for the symplectite formation. One hundred symplectic intergrowths were studied

to ascertain the presence or absence of oxide grains adjacent to the symplectite. Eighty intergrowths were found adjacent to discrete oxide grains; in twenty intergrowths no oxide-symplectite relationship could be found. The absence of discrete oxide in twenty out of one hundred cases can be explained in two ways. The oxide grain may exist nearby in the rock sample, but not be represented in the plane of the thin section. Alternatively, if the discrete oxide grain does take an active role in the olivine reaction to form orthopyroxene-oxide symplectite, there would presumably be cases where the oxide reactant would be completely consumed. Thus, no evidence for its former existence adjacent to the symplectite would be preserved.

The occurrence of discrete oxide grains adjacent to the orthopyroxene-oxide symplectite in 80% of the samples studied, the common occurrence of symplectic intergrowths within the olivine grains in the areas adjacent to discrete oxide grains, and the increase in the size of vermicules towards the oxide grain indicate that the discrete oxide grains, as well as the olivine grains, were associated with the reaction to form the symplectic intergrowths.

Symplectic intergrowths from 4 polished thin sections were studied to determine if a consistent ratio of orthopyroxene to oxide exists within a rock sample, or within symplectites as a group. Photographs of ten symplectic intergrowths, five from OPC and five from OCPC, were taken and each was enlarged to fill an 8-10 inch print. Two sizes of point grids were then placed over the photograph for point counting. The size of grid used was determined by the spacing between the

intergrowth components. Following the suggestion of van der Plas and Tobi (1965), the spacing between points counted was kept larger than the largest granule of the specimen. Most of the symplectites contained oxide vermicules oriented in linear trends in areas of the intergrowth; the grid was oriented at a 30° angle to the trend to prevent bias in counting. Only the areas containing oxide were considered, and the oxide-free rim was not included in the count.

The symplectic intergrowths of both the OPC and OCPC rock types maintained a very consistent ratio of oxide to orthopyroxene (Table 2). The mean volume % ratio of oxide to orthopyroxene is 30.1:69.9, with a standard deviation of 1.8. All symplectites studied fall within two standard diviations of the mean.

Oxide intergrowths in pyroxene. The Concord gabbro contains pyroxenes with oriented inclusions of oxide minerals. Similar pyroxene-oxide textures have been reported from other mafic complexes: oriented magnetite inclusions by Elsdon (1971), McSween (1980), and Fleet (1980) and oriented ilmenite inclusions by Schulze et al. (1978), Garrison and Taylor (1981), and Otten (1983). The formation of such oriented inclusions has generally been attributed to exsolution from a high temperature pyroxene. In the Concord gabbro, this texture occurs in all rock types, but is found in the greatest abundance in the OCPC samples. It was not observed in the clinopyroxene of the syenite. The oxide inclusions occur mainly as thin rods in both orthopyroxene (Fig. 11A) and clinopyroxene (Fig. 11B), oriented in one or two directions. They also occur as elongate platelets. Both forms may

Table 2. Point counts of ten symplectic intergrowths to determine volume percent of magnetite and orthopyroxene.

Sample	Total Count	# Oxide	# Opx	Vol % oxide	Vol % Opx
OCPC CG-11	1000	276	724	27.6	72.4
OCPC CG-11	2044	568	1576	27.8	72.2
OCPC CG-11	1367	436	931	31.9	68.1
OCPC CG-33	2480	737	1743	29.7	70.3
OCPC CG-33	1255	409	846	32.6	67.4
OPC CG-73	2664	804	1860	30.2	69.8
OPC CG-73	2269	672	1597	29.6	70.4
OPC CG-73	1618	527	1091	32.6	67.4
OPC CG-9	2015	600	1415	29.8	70.2
OPC CG-9	2224	645	1579	29.0	71.0

	Standard deviation	Arithmetic mean	
		Vol % oxide	Vol% OPX
OCPC(N=5)	2.29	29.9	70.1
OPC(N=5)	1.39	30.2	69.8
OPC+OCPC(N=10)	1.79	30.1	69.9

Figure 11. Oxide exsolution in pyroxenes. Both photomicrographs in plane-polarized light. Bar scales represent 0.1 mm.

A. Rods and platelets of oxide minerals in orthopyroxene. Sample Cg-11.

B. Rods and platelets of oxide minerals in clinopyroxene. Rim of clinopyroxene grain is clear of exsolution. Sample Cg-5.

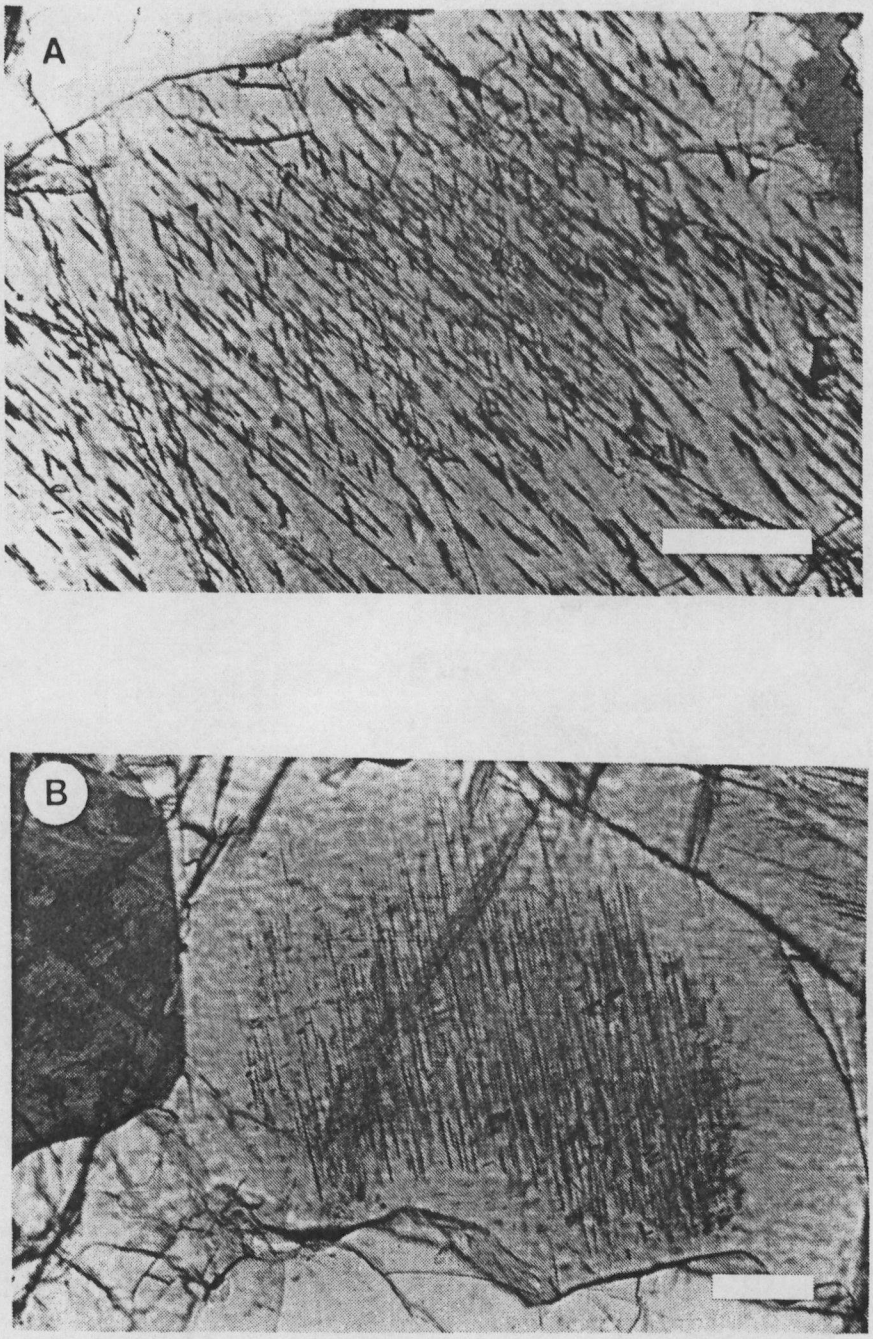

Figure 11 (continued)

occur in different orientations within a single pyroxene grain along the {010} plane. In most, but not all cases, the oxide rods and platelets tend to decrease in frequency as the pyroxene rim is approached (Fig. 11B). Whereas most of the oriented oxide inclusions in the pyroxenes appear to be magnetite, ilmenite inclusions do occur. In some cases ilmenite laths within magnetite rods and platelets can be seen. This suggests that titanomagnetite rods or platelets exsolved from the pyroxene at high temperatures, and then separated into magnetite and ilmenite phases on cooling.

CHAPTER IV

OXIDE MINERAL CHEMISTRY

Phase Compositions

Magnetite, ilmenite, hematite, and pleonaste have been analyzed with an automated MAC 400S electron microprobe using the correction procedures of Bence and Albee (1968) and the data of Albee and Ray (1970). The Fe^{3+} contents were calculated based on considerations of stoichiometry and charge balance. Because the oxide compositions are the result of complex oxidation and exsolution mechanisms, phases within each polished thin section and rock type commonly show significant compositional variation. Figure 12 illustrates the compositions of coexisting oxide minerals in the four rock types of the Concord complex.

Magnetite discrete grains. Representitive magnetite-ilmenite granule pairs of all gabbroic rock types are presented in Table 3. Minor elements in these pairs show consistant preferences for one of the two oxides phases. Partitioning coefficients for the magnetite-ilmenite pairs from Table 3 are presented on Table 4. Al_2O_3 and Cr_2O_3 are preferentally concentrated in magnetite, where as MnO and MgO are concentrated in ilmenite. Similar partitioning of these elements between magnetite and exsolved ilmenite composite grains have been documented in other studies (Elsdon, 1972; Czamanske & Mihalik, 1972; Neumann, 1974; Mathison, 1975; Haggerty, 1976; Thy, 1982).

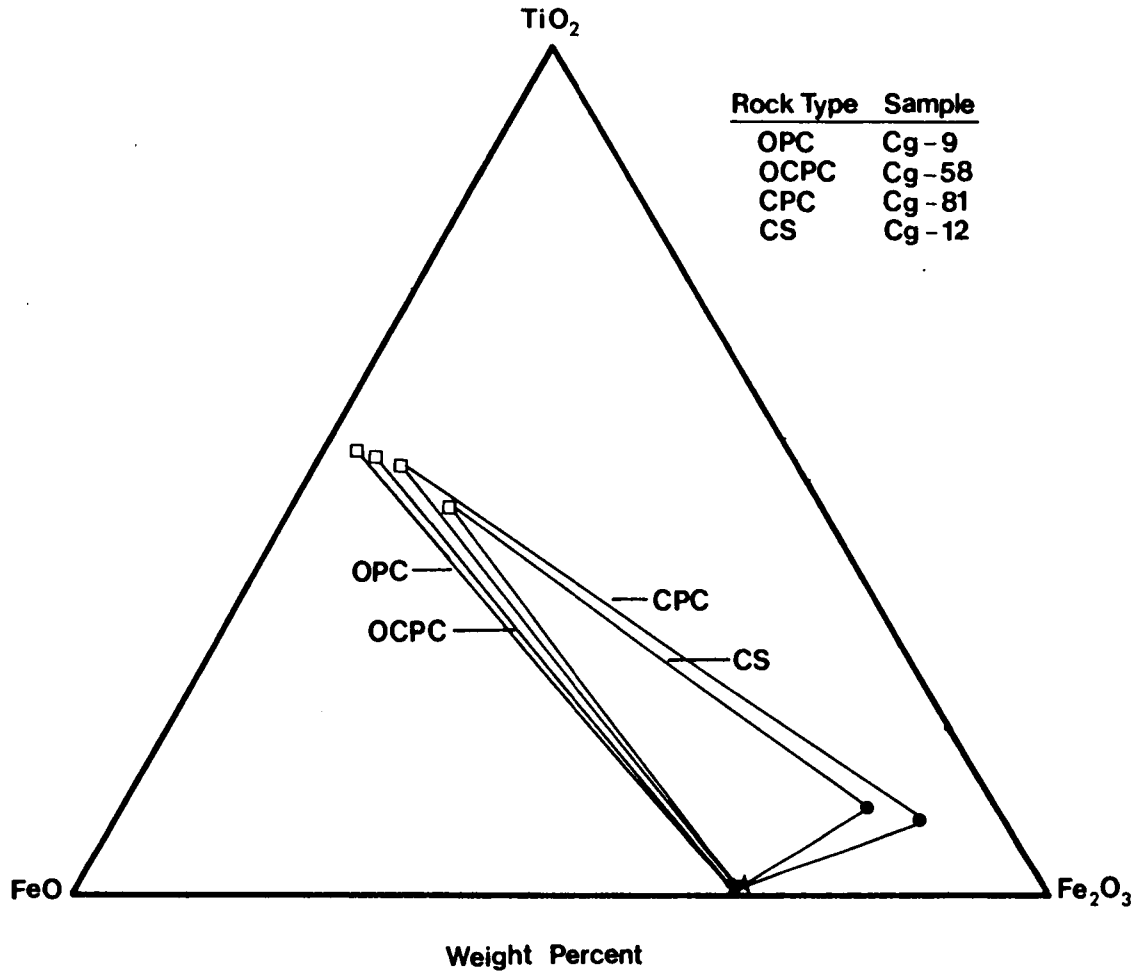

Figure 12. Phase chemistry of coexisting oxide minerals in the four rock types of the Concord igneous complex. Stars represent magnetite. Squares representilmenite. Circles represent hematite.

Table 3. Representative Microprobe Analyses of Associated Oxide Phases in Discrete Magnetite Grains.

	OPC Cg-9			OCPC Cg-58			CPC Cg-81	
	Magnetite[3*]	Ilmenite[6] Granule	Pleonaste[2] Bleb	Magnetite[3]	Ilmenite[3] Granule	Pleonaste[2] Bleb	Magnetite[3]	Ilmenite[3] Granule
Wt. % Oxide								
TiO_2	0.48 (10)	50.5 (6)	0.57 (13)	1.86 (5)	52.1 (3)	0.37 (2)	0.08 (5)	50.3 (4)
Al_2O_3	0.73 (6)	0.62 (2)	62.4 (4)	1.23 (6)	0.79 (3)	60.2 (6)	0.33 (2)	0.16 (1)
Cr_2O_3	0.52 (2)	0.04 (1)	0.80 (1)	0.43 (3)	0.01 (1)	0.79 (4)	0.34 (4)	0.02 (1)
Fe_2O_3#	66.6	4.85	0.62	64.4	3.38	5.18	67.3	5.82
FeO	31.6 (6)	38.2 (6)	18.0 (2)	31.2 (4)	40.4 (4)	16.5 (5)	31.2 (9)	38.4 (7)
MnO	0.14 (2)	1.21 (9)	0.27 (4)	0.14 (8)	1.00 (6)	0.04 (1)	0.01 (2)	3.10 (6)
MgO	0.32 (2)	3.56 (5)	15.6 (1)	0.46 (12)	2.83 (3)	16.6 (1)	0.16 (2)	1.92 (5)
TOTAL	100.39	98.98	99.26	99.72	100.51	99.63	99.34	99.72
Cation Basis	4	3	4	4	3	4	4	3
Ti	0.012	0.942	0.011	0.053	0.960	0.007	0.002	0.945
Al	0.024	0.019	1.945	0.055	0.023	1.863	0.015	0.005
Cr	0.011	0.001	0.016	0.012	0	0.016	0.010	0
Fe^{3+}	1.953	0.091	0.012	1.853	0.063	0.102	1.956	0.109
Fe^{2+}	0.987	0.790	0.399	0.997	0.829	0.363	1.008	0.803
Mn	0.006	0.025	0.006	0.004	0.021	0.001	0	0.066
Mg	0.007	0.132	0.611	0.026	0.104	0.648	0.009	0.072
TOTAL	3.000	2.000	3.000	3.000	2.000	3.000	3.000	2.000

#Fe^{3+} = Total Fe is reported as FeO, Fe^{3+} calculated by stoichiometry.
* = Number of replicate analyses.
Units in ( ) represent one standard deviation in terms of least units cited.

Table 4. Partitioning Coefficients Calcualted from Microprobe Analyses Given in Appropriate Tables.

A. Ratio of oxide weight % between magnetite and associated ilmenite. Data taken from Table 3.

	OPC, Cg-9	OCPC, Cg-58	CPC, Cg-81
Al_2O_3	1.18	1.56	2.06
Cr_2O_3	N.D.	N.D.	N.D.
MnO	0.12	0.14	N.D.
MgO	0.09	0.16	0.08

B. Ratio of oxide weight % between ilmenite and exsolved hematite. Data taken from Table 5.

Al_2O_3	0.71	0.53	1.77	2.11
Cr_2O_3	0.55	0.40	N.D.	N.D.
MnO	9.57	3.36	15.6	17.97
MgO	6.09	16.9	N.D.	N.D.

N.D. = Not detected, or one componant of ratio less than 0.04%.

Pleonaste. Representitive compositions of coexisting magnetite, ilmenite and pleonaste blebs are presented on Table 3. Although pleonaste represents only a small percentage of each magnetite grain, its composition must be considered in light of the magnetite-ilmenite partitioning. Both Al_2O_3 and Cr_2O_3 are preferentially concentrated in pleonaste, accentuating the partitioning trend between magnetite and ilmenite. The abundance of MgO in pleonaste suggests that there was a less strong preference of MgO to enter the exsolving ilmenite than the present magnetite and ilmenite compositions would seem to indicate.

Ilmenite-Hematite. Representative compositions of ilmenite and hematite pairs of the CPC gabbro and syenite are presented on Table 5. Partitioning coefficients for the ilmenite-hematite pairs from Table 5 are presented on Table 4. Both MnO and MgO show a definite preference for ilmenite in both rock types. No consistant partitioning trends are apparent for the small concentrations of Al_2O_3 and Cr_2O_3.

Symplectic intergrowths. The oxide phases, both magnetite and ilmenite, form vermicules in the symplectic intergrowths and have similar compositions as the same phases in the associated discrete grains. Table 6 compares the composition of similar phases in the symplectite and nearby discrete grains. The magnetite and ilmenite compositions of the symplectic vermicules are similar to the magnetite and ilmenite compositions of discrete grains in the same rock.

Table 5. Representative Microprobe Analyses of Ilmenite and Associated Hematite Lenses.

	CPC				CS			
	Cg-106A		Cg-81		CS-12		CS-21	
	Ilmenite[3*]	Hematite[3]	Ilmenite[3]	Hematite[2]	Ilmenite[4]	Hematite[3]	Ilmenite[4]	Hematite[2]
Wt. % Oxide								
TiO_2	49.9 (3)	11.7 (3)	48.9 (3)	9.12 (5)	51.2 (2)	10.7 (3)	52.5 (2)	10.6 (1)
Al_2O_3	0.12 (2)	0.17 (2)	0.10 (2)	0.19 (1)	0.16 (2)	0.09 (1)	0.19 (2)	0.09 (1)
Cr_2O_3	0.12 (2)	0.22 (4)	0.12 (3)	0.30 (1)	NA	NA	NA	0 (1)
$+Fe_2O_3$#	7.00	77.1	8.95	81.7	2.56	81.0	1.17	79.4
FeO	38.7 (7) 9146 (10)		9.3 (8)	7.27 (7)	39.7 (4)	9.01 (12)	41.2 (3)	9.03 (2)
MnO	0.67 (7)	0.07 (2)	0.47 (6)	0.14 (9)	5.91 (14)	0.38 (5)	5.75 (20)	0.32 (1)
MgO	3.11 (4)	0.51 (1)	2.37 (2)	0.14 (1)	0.22 (2)	0.05 (1)	0.23 (3)	0.01 (1)
TOTAL	99.62	99.23	100.21	98.86	99.75	101.23	101.04	99.45
Cation Basis	3	3	3	3	3	3	3	3
Ti	0.928	0.232	0.915	0.180	0.973	0.209	0.984	0.207
Al	0.004	0.005	0.003	0.006	0.005	0.003	0.006	0.003
Cr	0.002	0.005	0.002	0.006	NA	NA	NA	0
Fe^{3+}	0.131	1.529	0.168	1.635	0.149	1.582	0.022	1.586
Fe^{2+}	0.806	0.208	0.815	0.163	0.838	0.196	0.859	0.196
Mn	0.014	0.001	0.010	0.003	0.127	0.008	0.121	0.007
Mg	0.115	0.020	0.087	0.006	0.008	0.002	0.008	0
TOTAL	2.000	2.000	2.000	2.000	2.000	2.000	2.000	2.000

NA = Not analyzed.
#Fe^{3+} = Total Fe is reported as FeO, Fe^{3+} calculated by stoichiometry.
* = Number of replicate analyses.
Units in ( ) represent one standard deviation in terms of least units cited.

Table 6. Microprobe Analyses of Oxide Vermicules in Symplectites and Associated Discrete Oxide Grains.

	OCPC-Cg5				OCPC-Cg11			
	Magnetite		Ilmenite		Magnetite		Ilmenite	
	Vermicule[3*]	Discrete Grain[2]	Vermicule[3]	Discrete Grain[3]	Vermicule[2]	Discrete Grain[3]	Vermicule[2]	Granule[3]
Wt. % Oxide								
TiO_2	1.53 (6)	1.58 (2)	49.3 (7)	49.5 (1)	0.40 (3)	0.27 (8)	50.6 (5)	50.4 (6)
Al_2O_3	0.87 (9)	0.97 (4)	0.22 (2)	0.21 (4)	0.36 (2)	0.42 (4)	0.22 (2)	0.18 (2)
Cr_2O_3	0.26 (2)	0.22 (4)	0.07 (1)	0.04 (4)	0.32 (7)	0.40 (3)	0.08 (4)	0.10 (1)
Fe_2O_3#	65.9	64.4	8.02	8.35	66.3	67.9	5.61	6.17
FeO	32.6 (4)	31.9 (15)	37.3 (15)	36.5 (9)	30.8 (9)	30.9 (10)	37.0 (2)	37.2 (3)
MnO	0.22 (1)	0.21 (5)	1.36 (11)	1.43 (15)	0.10 (2)	0.04 (3)	1.12 (3)	0.93 (4)
MgO	0.45 (2)	0.25 (1)	3.59 (9)	3.43 (2)	0.23 (2)	0.19 (3)	4.04 (4)	4.16 (7)
TOTAL	101.83	99.53	99.86	99.46	98.51	100.12	98.67	99.14
Cation Basis	4	4	3	3	4	4	3	3
Ti	0.046	0.046	0.913	0.918	0.012	0.008	0.944	0.937
Al	0.038	0.044	0.006	0.006	0.017	0.019	0.007	0.005
Cr	0.007	0.007	0.001	0.001	0.010	0.012	0.002	0.002
Fe^{3+}	1.856	1.858	0.149	0.157	1.944	1.957	0.105	0.115
Fe^{2+}	1.021	1.023	0.771	0.761	1.001	0.991	0.768	0.768
Mn	0.007	0.007	0.028	0.030	0.003	0.001	0.024	0.020
Mg	0.025	0.014	0.132	0.127	0.013	0.011	0.150	0.153
TOTAL	3.000	3.000	2.000	2.000	3.000	3.000	2.000	2.000

#Fe^{3+} = Total Fe is reported as FeO, Fe^{3+} calculated by stoichiometry.
* = Number of replicate analyses.
Units in ( ) represent one standard deviation in terms of least units cited.

Zoning

In some studies, zoning has been recorded in individual oxide grains, and compositional differences have been found between primary and secondary ilmenite grains within the same sample (e.g., Duchesne, 1972; Mathison, 1975; Haggerty, 1976). Other studies have found no compositional difference between primary and secondary ilmenite phases (e.g., Elsdon, 1972; Haggerty, 1976; Himmelburg and Ford, 1977; Thy, 1982), and no compositional zoning within individual oxide grains, except at the magnetite-ilmenite shared boundary of the composite grains.

In the Concord complex, the only noticeable zoning occurs in the ilmenite grains at shared boundaries between ilmenite and magnetite or ilmenite and sulfide. Ilmenite grains with hematite exsolution show visible zoning near the contact of both magnetite and sulfide grains. At a distance of 20-70 um from the shared boundary, the hematite lenses begin to decrease in both size and number, leaving only homogeneous ilmenite at the border (Figs. 6A, C, D, pp. 17-18). This zoning does not occur when ilmenite shares a grain boundary with silicates or other ilmenite grains. Duchesne (1970, 1972) and Thy (1982) suggest that hematite-free rims in ilmenite adjacent to magnetite may be the result of the subsolidus reaction (Foslie, 1928)

$$Fe_2O_3 + Fe_2TiO_4 = FeTiO_3 + Fe_3O_4 \quad (1)$$

in which Fe_2TiO_4 and Fe_2O_3 are components of the magnetite and ilmenite, respectively.

On the other hand, Anderson (1966) and Kretchsmar and McNutt (1971) proposed that the hematite-free rim is the result of oxy-exsolution of ulvöspinel in the magnetite to ilmenite and its subsequent migration to adjacent ilmenite. According to Kretchsmar and McNutt (1971), the added ilmenite has the same composition as the ilmenite grain due to the buffering of fO_2 by the coexisting magnetite and ilmenite grains. Ramdohr (1980) has also noted this zoning of hematite lenses in ilmenite grains next to pyrrhotite when magnetite was not present; however he did not address the mechanism of formation.

Zoning was present in the ilmenite granule of the composite magnetite-ilmenite grain. The rim of the ilmenite granule sharing a common border with the magnetite granule was consistently higher in Ti and lower in Fe^{3+} than its core. The zoning did not occur near grain boundary contacts between adjacent ilmenite grains or ilmenite-silicate grains. This chemical zonation in ilmenite near the magnetite-ilmenite composite border is represented visually by the progressive decrease and disappearance of the hematite exsolution in this area. In visually homogeneous ilmenite, electron microprobe data showed similar zoning in ilmenite at the magnetite boundary. The companion magnetite granule, however, did not show noticeable complimentary zoning at the common border. Microprobe analyses indicating the presence of zoning are given in Table 7. Himmelberg and Ford (1977) and Mathison (1975) found that magnetite was zoned and showed a decrease in Ti and an increase in Fe as the ilmenite granule or internal ilmenite laths were approached. This anticipated reciprocal zonation of magnetite granules was not found in

Table 7. Representative Microprobe Analyses of Zonation in Ilmenite Next to Magnetite.

	OPC-Cg 74 Ilmenite		OCPC-Cg 58 Ilmenite		CPC-Cg 81 Ilmenite		CS 21 Ilmenite	
	Core[4*]	Rim[3]	Core[3]	Rim[2]	Core[3]	Rim[3]	Core[3]	Rim[3]
Wt. % Oxide								
TiO_2	48.8 (4)	51.3 (9)	52.1 (1)	54.5 (3)	49.1 (2)	52.3 (2)	52.1 (7)	53.2 (4)
Al_2O_3	0.88 (13)	0.74 (2)	0.79 (4)	0.90 (2)	0.11 (1)	0.12 (1)	0.17 (1)	0.17 (1)
Cr_2O_3	NA	NA	NA	NA	0.07 (1)	0.03 (1)	NA	NA
$+Fe_2O_3$#	8.34	4.24	3.38	0	7.49	2.36	1.89	0
FeO	36.6 (3)	38.6 (6)	40.4 (2)	41.0 (3)	8.2 (6)	40.3 (1)	40.8 (8)	40.4 (6)
MnO	1.39 (6)	1.61 (5)	1.00 (5)	1.13 (4)	2.32 (7)	2.57 (11)	5.67 (6)	6.36 (9)
MgO	3.41 (3)	3.33 (3)	2.83 (2)	2.92 (1)	2.54 (3)	2.75 (3)	0.28 (1)	0.23 (4)
TOTAL	99.42	99.82	100.50	100.45	99.83	100.43	100.91	100.36
Cation Basis	3	3	3	3	3	3	3	3
Ti	0.907	0.950	0.960	1.009	0.920	0.970	0.978	1.004
Al	0.026	0.022	0.023	0.026	0.003	0.003	0.005	0.005
Cr	NA	NA	NA	NA	0.001	0	NA	NA
Fe^{3+}	0.155	0.079	0.063	0	0.140	0.043	0.036	0
Fe^{2+}	0.757	0.793	0.829	0.837	0.794	0.830	0.853	0.846
Mn	0.029	0.034	0.021	0.023	0.049	0.053	0.120	0.136
Mg	0.126	0.122	0.104	0.105	0.094	0.101	0.008	0.008
TOTAL	2.000	2.000	2.000	2.000	2.000	2.000	2.000	2.000

NA = Not analyzed.
#Fe^{3+} = Total Fe is reported as FeO, Fe^{3+} calculated by stoichiometry.
* = Number of replicate analyses.
Units in ( ) represent one standard deviation in terms of least units cited.

the Concord magnetite. The absence of compositional zoning may be due to the complicated subsolidus history of the magnetite.

The simple magnetite zonation that occurred at the ilmenite granule border may have been destroyed as a second and third period of ilmenite oxydation-exsolution took place. The formation of abundant smaller ilmenite lamellae would have left a much smaller scale of zonation overprinted on the magnetite granule. After three periods of zonation due to ilmenite exsolution, any zonation of the magnetite granule would be difficult to detect.

Primary Igneous Trends Preserved in Oxide Compositions

Silicate minerals of the Concord gabbro (Olsen et al., 1983) indicate increasing differentiation in the rock types OPC, OCPC, CPC, and syenite, based on iron enrichment of ferromagnesian minerals and Na enrichment in plagioclase cores. Magnetite was formed under conditions of high water content and accompanying elevated fO_2 as evidenced by early crystallization of magnetite (Osborn, 1962; Hamilton et al., 1964; Elsdon, 1972; McSween and Nystrom, 1979) and modal increase of the hydrous minerals within the gabbro (Olsen,1982). Replacement of orthopyroxene by hornblende and magnetite by biotite indicate the presence of a late stage aqueous fluid. The composition and textures in the Concord rock suite are the result of complex oxidation, exsolution and subsolidus reequilibration facilitated by the high water content of the melt. Thus, apparent trends of the element oxides with increasing fractionation must be studied carefully. Compositional trends may be affected by partitioning between exsolved oxide pairs, the changing

composition and crystallization conditions of fractionation, and the degree of reequilibration. Variation diagrams of element wt % of magnetite and ilmenite clearly show compositional trends of both the major (Fig. 13) and minor elements (Fig. 14) in the Concord suite. Because of low concentrations, the variation diagrams of MnO for magnetite and Cr_2O_3 for ilmenite are omitted. These trends are similar to those found in oxides of other differentiated complexes (e.g., Vincent and Phillips, 1954; Duchesne, 1972; Mathison, 1975; Himmelburg and Ford, 1977; Thy 1982) and may reflect melt fractionation.

The magnetite of the OPC is represented by two sets of data. One set contains probe analysis of magnetite grains disseminated throughout the rock, similar in textures and mineral assemblages to the magnetite grains of all other rock types. The second set consists of analyses of subhedral magnetite grains surrounded by cumulus olivine. These two kinds of magnetite, formed from the same melt, allow the comparison between grains that cooled slowly and reequilibrated in the presence of elevated fO_2, and those grains that also cooled slowly but were isolated from the effects of late-stage magmatic fluids. The magnetite composition of grains in the cumulus olivine accentuate the trends (except for Cr_2O_3) that are formed by the remaining magnetite grains not surrounded by a cumulus phase.

The contents of MgO show a steady decrease in both magnetite and ilmenite. MgO is preferentially partitioned into ilmenite. While the magnetite trend may be affected by a greater degree of ilmenite exsolution with increased fO_2, the ilmenite trend reflects the decrease

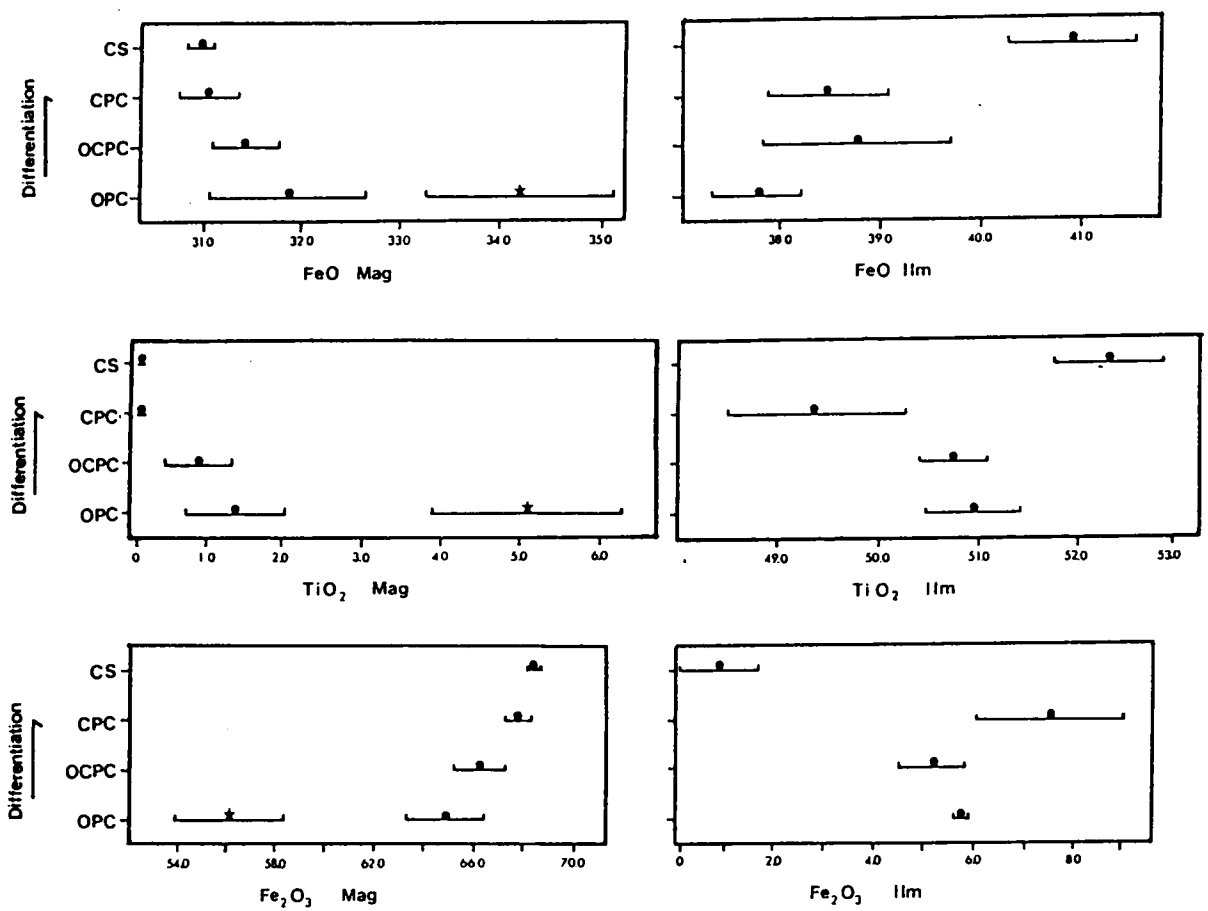

Figure 13. Variation diagrams of the major elements in magnetite (Mag) and ilmenite (Ilm) with different rock types. The stars represent compositions of subhedral magnetite grains surrounded by cumulus olivine.

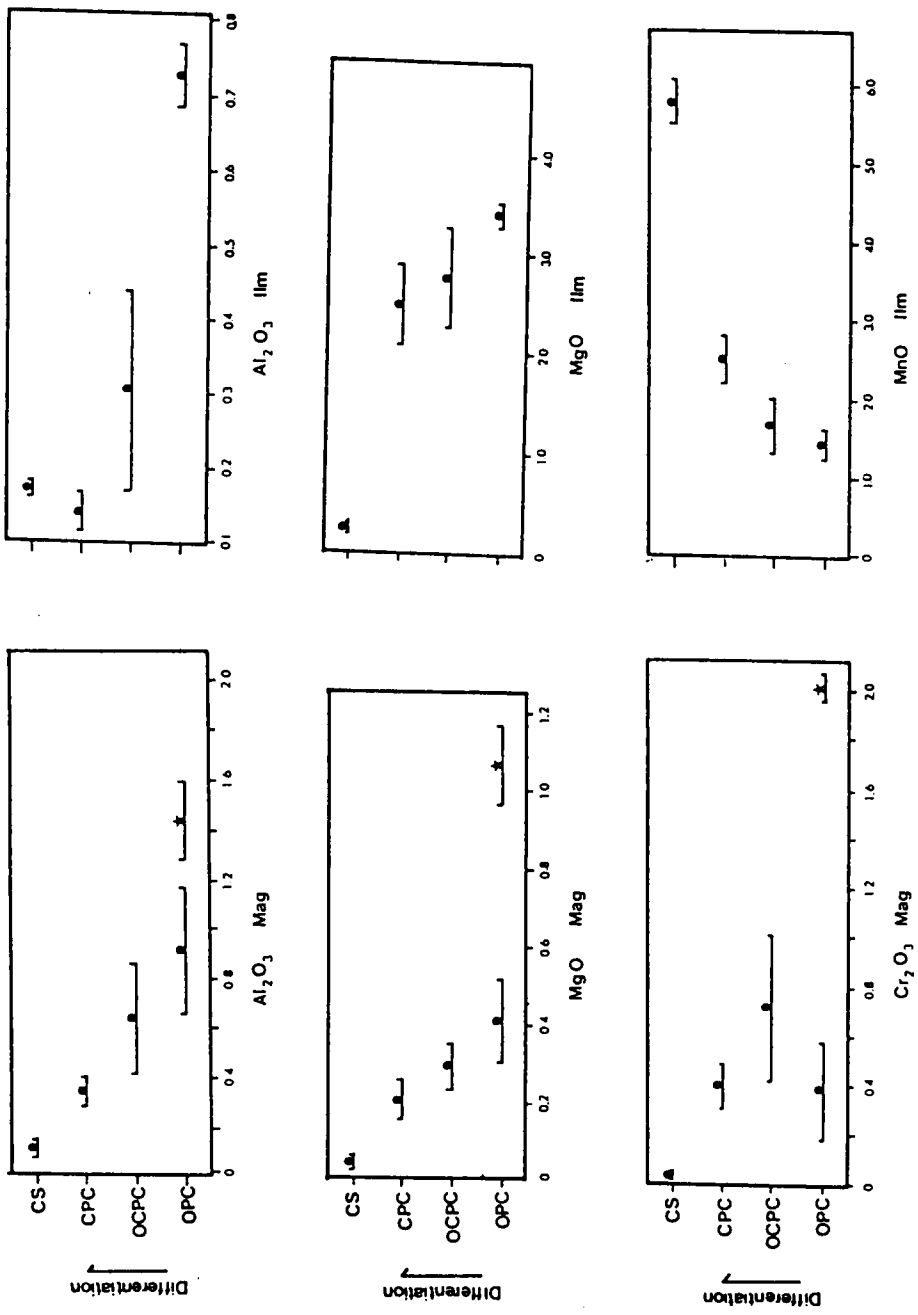

Figure 14. Variation diagrams of the minor elements in magnetite (Mag) and ilmenite (Ilm) with different rock types. The stars represent compositions of subhedral magnetite grains surrounded by cumulus olivine.

in MgO of the melt with differentiation that is also found in the ferromagnesian silicate minerals (Olsen,1982). Magnetite contains very small amounts of MnO due to the partitioning of MnO into ilmenite and the increased degree of exsolution. MnO in ilmenite shows a steady increase throughout the rock types. This trend may reflect the preference of the ilmenite structure for Mn^{2+} that increases with decreasing temperature (Buddington and Lindsley, 1964; Neumann, 1974), as well as the differentiation index of the host rock (Czamanske and Mihalik, 1972; Neumann, 1974; Thy, 1982).

The contents of Al_2O_3 in magnetite and ilmenite decrease steadily, with the exception of a slight rise of low concentration in the syenite. Because Al_2O_3 is partitioned into magnetite, the overall trend of decreasing Al_2O_3 in magnetite and ilmenite reflects the changing composition and crystallization conditions of the magma as suggested by Haggerty (1976) and Himmelburg and Ford (1980). Cr_2O_3 was strongly partitioned into magnetite, thus accounting for its extremely low concentration in ilmenite. In magnetite, Cr_2O_3 shows an increase from OPC to OCPC, then a steady decrease through the syenite. The magnetite within the cumulus olivine grain shows over five times as much Cr_2O_3. Cr_2O_3 preferentally enters pleonaste. However, exsolved pleonaste is present in all magnetite of the OPC, OCPC, and CPC samples. It is unclear why the magnetite of the OPC contains less Cr_2O_3 than that of the OCPC or the CPC.

The major element concentrations of magnetite and ilmenite are governed by oxidation exsolution, a result of relative increases in fO_2.

Magnetite shows a steady increase in Fe_2O_3, reflecting the elevated fO_2 and the iron-enrichment trend. As expected, FeO decreases with increase in Fe_2O_3. TiO_2 in magnetite also steadily decreases, approaching concentrations below detection limits in the CPC gabbro, as ilmenite is increasingly more completely exsolved. The major elements in ilmenite show the same interrelationship, with FeO mirroring Fe_2O_3, and TiO_2 behaving similarly to FeO. The marked decrease in Fe_2O_3 in the ilmenite of the syenite reflects the greater depletion in hematite due to exsolution, as the second set of hematite lamellae exsolved forming the synneusis texture. Analysis of the ilmenite grains of the syenite with a defocused beam gives a range of Fe_2O_3 from 12 to 22%, indicating that both ilmenite and magnetite reflect the overall increasing oxidation trend of the magma.

High H_2O activity and elevated fO_2 conditions enhanced reequilibration in all of the rocks of the Concord suite. Nevertheless, minor elements in magnetite and ilmenite increase or decrease similarly within fractionation independant of preferential partitioning. Therefore, it is concluded that variation of minor elements in magnetite and ilmenite reflect the fractionation process of the magma. The trends are preserved, although the slopes of the trends have been altered by substantial reequilibration brought about by the high water activity of the magmas. The degree of this change is suggested by the compositional difference of the two sets of magnetite in the OPC gabbro. The trends of the major elements are controlled by elevated fO_2 conditions and increasing degree of exsolution.

CHAPTER V

PETROGENESIS OF OXIDE MINERALS

The cumulus and interstitial oxide grains occur in euhedral to anhedral forms. The interstital texture of many anhedral grains, together with the virtual lack of intergrowth textures between oxides and sulfides, suggest that the oxide minerals crystallized from a silicate melt and not from an immiscible sulfide-oxide melt.

The formation of phases in the melt and their subsequent subsolidus history is schematically presented in Figure 15. This figure may be referred to throughout this discussion to facilitate understanding of the crystallization history.

Magnetite

Magnetite began to crystallize early as cumulus grains and continued to crystallize throughout the formation of the complex, as both cumulus and interstitial grains.

The anhedral grains may have resulted from early formed cumulus grains that were favorably positioned in or near intercumulus liquid, so as to provide nucleation sites for the adcumulus oxides within the interstitial area (Wright, 1961; Elsdon, 1972); or, as suggested by Mathison (1975) and Thy (1982), the cumulus grains formed early, and the anhedral grains formed later than the cumulus minerals from the remaining interstitial liquid. Both methods of formation would produce subhedral cumulus and anhedral interstitial grains. There is no clear zoning or compositional difference between these grain types to support

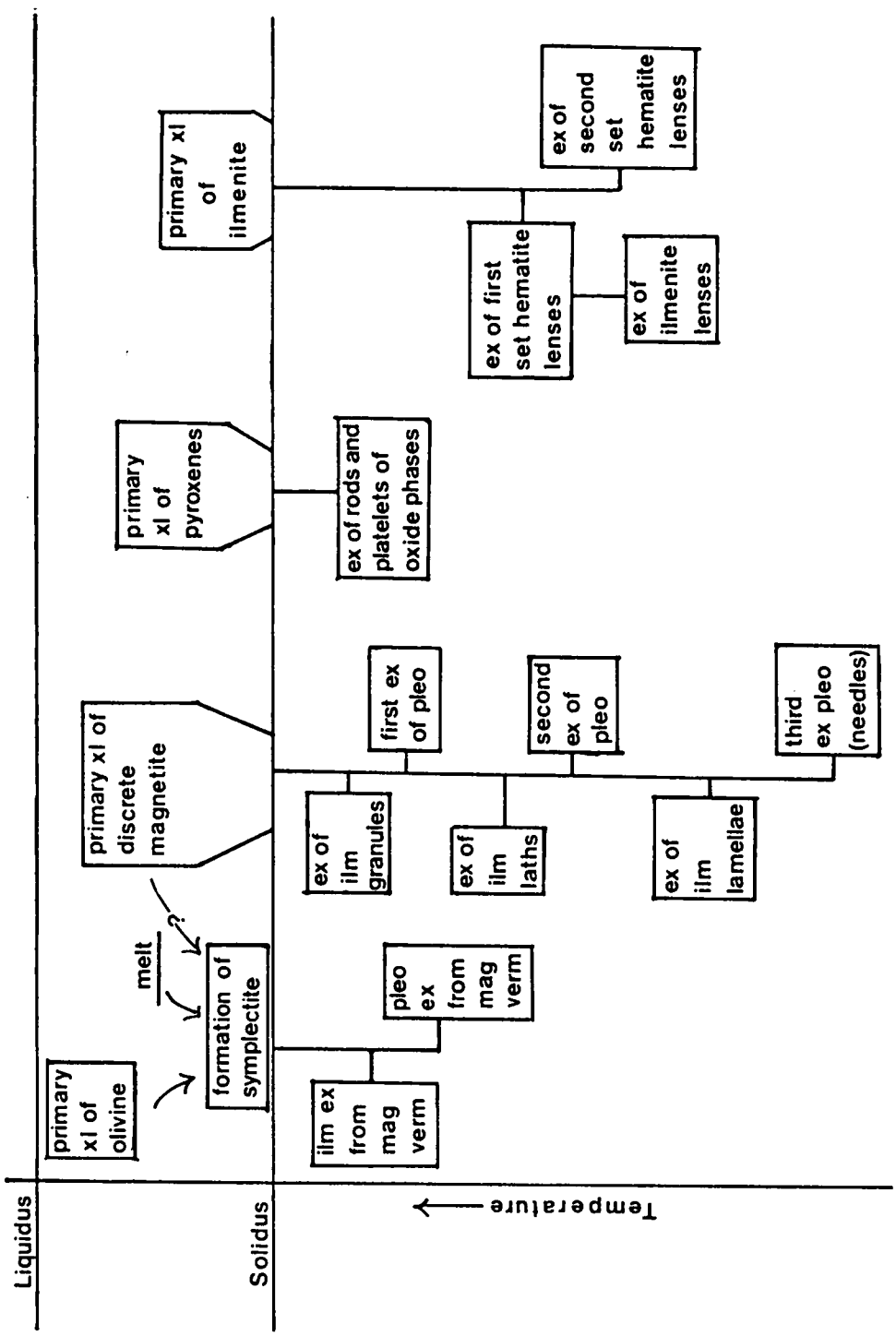

Figure 15. Schematic diagram of the crystallization history in the Concord complex. The timing of subsolidus reactions between different primary phases is unknown. Xl = crystallization. Ex = exsolution. Ilm = ilmenite. Pleo = pleonaste. Verm = vermicules.

either hypothesis. The anhedral oxide grains are significantly larger than cumulus magnetite grains.

There are few discrete ilmenite grains in the OPC and CPC samples. This suggests that cumulus magnetite, later exsolving ilmenite, was the first oxide mineral to crystallize. Because the integrity of the small regular grains was maintained, little or no adcumulus ilmenite or magnetite appears to have been added. Both magnetite and ilmenite discrete grains then began crystallizing in the interstital spaces with increased fractionation.

Ilmenite Exsolution

Co-precipitation (e.g., Heier, 1956; Duchesne, 1972; Haggerty, 1976) and granule exsolution (e.g., Buddington and Lindsley, 1964; Himmelberg and Ford, 1977; Thy, 1982; Von Gruenwaldt et al., 1985) are the dominant hypotheses proposed in the literature to explain the granular magnetite-ilmenite texture of the discrete magnetite grains. In the Concord gabbro, the textural gradation between internal sandwich laths and external ilmenite granules, together with the low abundance of ilmenite discrete grains in the OPC and OCPC samples suggest that external ilmenite granules were formed by oxidation-exsolution.

It is difficult to distinguish between large internal sandwich laths at or near the rim of a magnetite grain and an external ilmenite granule. Pleonaste may occur as needles or small blebs throughout the internal sandwich laths and as blebs at the magnetite borders of the ilmenite granules. Two shared boundaries of magnetite-ilmenite granules may be parallel to the internal ilmenite exsolutions of the magnetite

granules. The gradation between internal ilmenite laths and external granules reflect a similar process of formation, interpreted as oxidation-exsolution. Ilmenite and magnetite co-precipitating in the magma would tend to produce discrete grains of ilmenite, as well as discrete grains of magnetite. The scarcity of ilmenite discrete grains in the OPC and OCPC samples that contain grains with ilmenite granules further indicates that oxidation-exsolution and not co-precipitation was the mechanism of formation for the ilmenite granules.

The ilmenite granules, laths, and trellis lamellae appear to have formed by the same oxidation-exsolution process at sucessively lower temperatures, as suggested originally by Buddington and Lindsley (1964). The formation of external granular ilmenite predates the internal ilmenite exsolution features found in magnetite. Internal ilmenite textures formed as the more restricted diffusion rates at lower temperatures prevented the exsolved ilmenite from migrating to the grain boundary. Ilmenite remained in the host as laths, or at lower temperature, as lamellae, oriented parallel to the {111} planes of magnetite.

Pleonaste Exsolution

Pleonaste is associated with the magnetite of the Concord gabbro and is absent in the magnetite of the syenite. Its occurrences as blebs at or near the magnetite grain boundaries and as needles within the magnetite suggest that there were at least two and possibly three periods of pleonaste exsolution. Similar pleonaste textures have been observed in magnetite from other studies (Turnock and Eugster, 1962;

Anderson, 1966, 1968; Mathison, 1975; Haggerty, 1976; McSween and Nystrom, 1979; Price, 1979; Thy, 1982; Gruenewaldt, 1985).

In the Concord gabbro, there are two to three different stages of ilmenite oxidation-exsolution, and three different stages of pleonaste exsolution within the magnetite. The recurring textural association of pleonaste with ilmenite suggests that their exsolution from magnetite is interrelated. The pleonaste blebs occur at the magnetite-silicate border but still within the magnetite, and at the magnetite-ilmenite border actually within the ilmenite. Textural evidence suggests that this earliest generation of pleonaste began to exsolve at the end of the oxidation-exsolution of ilmenite to form the ilmenite granule. Diffusion rates allowed the pleonaste components to migrate outward to the magnetite boundaries. When this occurred simultaneously with the end of the first period of oxidation-exsolution of ilmenite, both ilmenite and pleonaste exsolved from the magnetite structure to form a rim of both ilmenite and pleonaste (Fig. 5A, pp. 12-13), as described by Duchesne (1970; 1972). Many ilmenite laths contain small blebs and needles of pleonaste either at the edges of the laths or disseminated throughout (Figs. 5C,E). This textural relationship suggests that the second stage of pleonaste exsolution was concurrent with the oxidation-exsolution to form ilmenite laths. Pleonaste also occurs as tiny needles throughout the magnetite. In cases where crosscutting relationships occur, the pleonaste needles crosscut the ilmenite lamellae, the third stage of ilmenite oxidation-exsolution (Fig. 5F). The

cross-cutting relationship indicates that the pleonaste needles postdate the formation of ilmenite lamellae.

The occurrence of pleonaste blebs at the magnetite-silicate boundaries, as well as the crystallographically oriented pleonaste needles within the magnetite are clear evidence that the pleonaste exsolved from the magnetite. The recurring association of pleonaste within ilmenite oxidation-exsolution textures indicates that the formation of both are related. Haggerty (1976) suggested that the formation of pleonaste with magnetite is an "imposed" exsolution brought about by the supersaturation of Al_2O_3 in the magnetite. Indeed, aluminium is preferentially partitioned into the magnetite as ilmenite is formed by oxidation-exsolution (Mathison, 1975; Haggerty, 1976; Himmelburg and Ford, 1977). As saturation of Al in the magnetite occurs, pleonaste begins to exsolve. This mechanism for imposed exsolution of pleonaste in magnetite is supported by the textural evidence of pleonaste and ilmenite in the magnetite grains of the Concord gabbro, i.e., the consistent relationship of one stage of pleonaste exsolution apparently occurring near the end or just after one stage of ilmenite exsolution. With each stage of ilmenite exsolution, aluminium was partitioned into the magnetite phase, saturating the magnetite and promoting pleonaste formation. Each stage of exsolution occurred at a lower temperature, therefore with lower diffusion rates. The earliest stage of pleonaste exsolution occurred when diffusion rates allowed the pleonaste to migrate outward and form blebs at the magnetite boundary. The diffusion rates during the last stage of

pleonaste exsolution allowed only the formation of needles oriented along the {100} planes of magnetite where they remain disseminated throughout the grain.

Hematite Exsolution

Hematite occurs as one or two generations of oriented lenses within ilmenite. As their crystallographic orientations within the ilmenite would suggest, the hematite lenses are formed by exsolution from the ilmenite host. The larger lenses were formed earlier than the similarly oriented, smaller, second generation lenses of the synneusis texture. Their size, abundance, and the presence of one or two generations of exsolution lamellae are directly related to the hematite content within the ilmenite (Basley and Buddington, 1958; Duchesne, 1970). Several studies have correlated the varying exsolution textures occurring between hematite and ilmenite with the approximate mol % hematite (e.g., Duchesne,1970; Kretchsmar and McNutt,1971).

In the Concord rock suite, microprobe analyses with a defocused beam show similar comparisons of hematite exsolution textures in ilmenite with increasing hematite content. The visually homogenous ilmenite of the OPC and OCPC rocks contain 4-6 mol % hematite. Ilmenite of the CPC and syenite samples that contain a single set of hematite exsolution lenses have 8-11 mol % hematite. The synneusis texture is found in the syenite where ilmenite contains 15 to 21 mol % hematite. This is in close agreement with Kretchmar and McNutt (1971), who found that exsolution in ilmenite producing two sets of hematite lenses begins at about 15 mol % hematite. This pattern follows the iron-enrichment

differentiation trend in the Concord complex (Olsen et al., 1983). The exsolution textures of the hematite appear to be indicative of the iron-enrichment trend and increased oxidation within the ilmenite grain, which reflects the enrichment trend of the whole rock suite.

Symplectic Intergrowths

The origin of the unique texture displayed by the symplectic intergrowths must explain several parameters:

1. the identical chemistry of the oxide phases occurring in both discrete grains and vermicules within the intergrowths;
2. the similar composition of the orthopyroxene both within the symplectite and as poikilitic grains not associated with this texture;
3. the association of symplectic intergrowths with olivine;
4. the association of the symplectic intergrowths with discrete oxide grains;
5. the coarsening of the vermicules away from the olivine contact and towards the associated discrete oxide grain;
6. the relative chemistries of the olivine, orthopyroxene, and the oxide phases; and
7. the constant volume ratio within the symplectites of orthopyroxene:oxide phases-70:30;
8. the distinctly different ratios of magnetite to ilmenite in the vermicules of symplectic intergrowths within a single polished thin section.

A popular interpretation of the origin of this intricate texture involves the oxidation of olivine (Muir et al., 1957; Haggerty and Baker, 1967; Goode, 1974; Esbensen, 1978; Otten, 1983). This origin is readily ruled out for the symplectic texture under discussion, based on the fact that the olivine does not have sufficient Fe, Ti, Al, or Ca to form the orthopyroxene or magnetite-ilmenite phases. Microprobe analysis of olivine, orthopyroxene, and magnetite from three olivine grains and the associated symplectites are given in Table 8. Indeed, based upon calculations shown in Table 9, it can be seen that the reaction to form this symplectite is not a "volume for volume" replacement of olivine. The loss of magnesium and large gain in iron are in agreement with the calculations of Ambler and Ashley (1977). It is obvious that the formation of symplectic intergrowths in the Concord gabbro is not caused by simple oxidation of olivine; rather, a significant introduction of chemical components is necessary.

Three hypotheses can possibly account for most of the observations:

1. the late-magmatic reaction of olivine with residual liquid (Ambler and Ashley, 1977; van Lamoen, 1979; McSween, 1980);
2. resorption of olivine with simultaneous precipitation of orthopyroxene and magnetite/ilmenite (Garrison and Taylor, 1981); and
3. reaction between olivine, early formed discrete oxide, and residual melt (this thesis).

The first hypothesis of reaction of olivine with residual melt does not seem to provide any explanation for why orthopyroxene and magnetite

Table 8. Representative Microprobe Analyses of Magnetite Vermicules and Orthopyroxene in Symplectic Intergrowths and Associated Olivine Grains. Mag. verm. = Magnetite Vermicule, OPX = orthopyroxene, ol = olivine.

	Cg 11 1B			Cg 11 3C		
	Mag 2* Verm.	OPX[3]	ol[4]	Mag[2] Verm.	OPX[3]	ol[4]
SiO_2	NA	53.3 (3)	3.78 (1)	NA	52.9 (3)	37.7 (1)
TiO_2	0.47 (15)	0.18 (3)	NA	0.40 (3)	0.22 (2)	NA
Al_2O_3	0.40 (1)	2.01 (2)	NA	0.36 (2)	2.09 (4)	NA
Cr_2O_3	0.39 (1)	NA	NA	0.32 (7)	NA	NA
Fe_2O_3#	67.5	NA	NA	66.3	NA	NA
FeO	30.8 (13)	15.5 (1)	23.0 (2)	30.8 (9)	14.3 (3)	22.7 (1)
MnO	0.17 (1)	0.41 (5)	0.41 (4)	0.10 (2)	0.43 (1)	0.42 (3)
MgO	0.26 (3)	27.4 (1)	39.3 (2)	0.23 (2)	28.7 (2)	39.3 (2)
CaO	NA	0.61 (1)	NA	NA	0.76 (11)	NA
TOTAL	99.9	99.41	100.51	98.51	99.40	100.12
Cation Basis	4	6	4	4	6	4
Si	NA	1.936	0.982	NA	1.913	0.982
Ti	0.014	0.004	NA	0.012	0.005	NA
Al	0.018	0.085	NA	0.017	0.088	NA
Cr_{3+}	0.012	NA	NA	0.010	NA	NA
Fe^{3+}	1.949	NA	NA	1.944	NA	NA
Fe^{2+}	0.985	0.470	0.500	1.001	0.433	0.495
Mn	0.006	0.012	0.008	0.003	0.013	0.009
Mg	0.015	1.482	1.523	0.013	1.545	1.526
Ca	NA	0.023	NA	NA	0.028	NA
TOTAL	3.000	4.012	3.013	3.000	4.025	3.012

* = Number of replicate analyses.

NA = Not analyzed.

Units in ( ) represent one standard deviation in terms of least units cited.

#Fe^{3+} = Total Fe is reported as FeO, Fe^{3+} calculated by stoichiometry.

Table 9. Calculation by weight of gains and losses of MgO, FeO, and SiO_2 (with excess oxygen) in an idealized reaction of olivine forming a magnetite-orthopyroxene symplectic intergrowth. Densities of 3.5 g/cm^3 for olivine, 3.4 g/cm^3 for orthopyroxene and 5.18 g/cm^3 for magnetite are used. Compositions are taken from the first symplectite found in Table 8. After Ambler and Ashley (1977).

	Ol	Opx	Mag	Total Sym	Difference	% Change
MgO	1.37	0.68	0.004	0.684	0.69 gm lost	50% wt. loss
*FeO	0.81	0.38	1.44	1.82	1.01 gm gain	125% wt. gain
SiO_2	1.32	1.32	-	1.3	0 gm	no change

*Total Fe as FeO

**3.50 gm (Fo_{75}) 2.38gm (En_{76}) + 1.55 gm (Fe_3O_4)

are formed rather than just pyroxene, as would normally be expected. It also does not explain the constant ratio of orthopyroxene and oxide with the variations in the oxide phases within the symplectite; nor does it explain the association of symplectites with discrete oxide grains. Although McSween (1980) suggested that the similar oxide compositions are due to the subsolidus reequilibration of all oxides to lower temperature, this is unlikely for distinct oxide grains that are not in physical contact. They might reequilibrate to similar fO_2 conditions, but could not exchange major cations, as would be necessary for complete reequilibration.

Garrison and Taylor (1981) used the pioneering work of Osborn (1962) to explain the formation of the symplectite. Phase equilibria in the system Mg_2SiO_4-Fe_3O_4-$CaSiO_3$-SiO_2 at moderately high oxygen fugacities contains a reaction surface for olivine which occurs simultaneously with the crystallization of orthopyroxene and magnetite. At the appropriately high fO_2, if the liquid path intersects the reaction surface bounding the fields of low-Ca pyroxene, olivine, and magnetite, the olivine will be resorbed whilethe orthopyroxene and magnetite form. If the reaction surface is not intersected, the olivine will not back-react, but the formation of orthopyroxene and magnetite will nonetheless continue. The crystallization of the orthopyroxene and magnetite will occur at a fixed ratio, a function of the bulk composition of the residual melt. The presence of Al and Ti in the melt will obviously influence the chemistries of the crystallizing phases, both within the intergrowth and as adjacent discrete grains. However, the

composition of the residual melt would have to be different within distances of only a few millimeters to a centimeter in order to explain the different ratios of magnetite to ilmenite found in the symplectites of a single thin section.

The unique texture of the symplectite would seem to involve the kinetics of nucleation and growth at and near the interface with the reacting olivine. The orthopyroxene and oxide formed during the early reaction of the olivine would have sufficient time to coarsen as the reaction works its way into the olivine. The discrete oxide may then be the result of continued reequilibration of this texture (L. A. Taylor, pers. comm.).

An alternative explanation for the formation of symplectites (#3 above) involves the reaction of olivine, early formed discrete oxide, and residual melt (as evidenced by poikilitic orthopyroxene or amphibole). This would explain the common occurrence of the discrete oxide and olivine with the symplectic intergrowth, as well as the similar chemistries of the oxide phases. The different ratios of magnetite to ilmenite in the vermicules of symplectic intergrowths would then be directly related to the phases of the previously formed discrete grains. The associated discrete oxide grains may have supplied the large amount of iron and titanium needed, and the residual melt would have provided the minor elements, as well as served as a sink for magnesium.

It is difficult to explain the consistant ratio of orthopyroxene to oxide phases in the symplectite when varing amounts of residual melt and oxide phases may be involved. The composition of the olivine is more

magnesium-rich in the Concord gabbro than in the Waterangs layered mafic intrusion as reported by Ambler and Ashley (1977). The volume percentage of iron oxide present in the symplectite is lower in the Concord gabbro (30%) than in the Waterangs intrusion (43%). This suggests there may be a possible relationship between the olivine composition and the abundance (volume %) of oxide and orthopyroxene in the symplectite. Alternatively, the differences in bulk chemistry of the melts, as reflected by the different olivine compositions, may well be the controlling factor. Other studies of olivine and replacing symplectic intergrowths will be necessary to resolve which mechanism best explains the symplectite formation and to determine what factor controls the modal proportions of the symplectite.

CHAPTER VI

CONCLUSIONS

1. Early formed cumulus magnetite with olivine and abundance of hydrous minerals reflect the high water activity and elevated fO_2 conditions of crystallizing magma.

2. High water activity and elevated fO_2 conditions encouraged reequilibration of the oxide compositions. Nevertheless, evidence of differentation is preserved in the compositions of the oxide minerals. Steady increases in the hematite content of ilmenite reflect limited iron enrichment with differentiation. Variations of the minor elements in both magnetite and ilmenite reflect a similar differentiation trend. The variation of the major elements were controlled by increasingly elevated fO_2 and increasing degree of exsolution.

3. Ilmenite was oxy-exsolved from magnetite, forming external and internal granules, laths, and lamellae. Each period of ilmenite exsolution was accompanied by an imposed exsolution of pleonaste in the magnetite, resulting in the ilmenite-pleonaste textures.

4. Hematite textures in ilmenite reflect increasing hematite content and the method of exsolution. Hematite was continuously exsolved from ilmenite below 15 mol % hematite, producing a single set of hematite lenses of uniform size. Above 15 mol % hematite, exsolution in ilmenite produced two sets of hematite lenses.

5. Symplectic intergrowths of orthopyroxene and magnetite-ilmenite vermicules usually occur at borders of olivine grains adjacent to

discrete oxide grains. Clear replacement textures indicate that olivine was partly replaced by symplectic intergrowths. The phases present in the symplectite vary with the phases of the associated oxide grain. Two possible mechanisms of symplectite formation account for the textural observations, phase compositions, and grain associations. First, the formation of symplectic intergrowth may have been caused by the co-precipitation of orthopyroxene and oxide phases while olivine was being resorbed by the melt. This would suggest that at a certain melt composition and/or fO_2, both orthopyroxene and oxide crystallized, forming the symplectic intergrowth while replacing olivine. A second possibility is that olivine, early formed discrete oxide, and melt (as evidenced by poikilitic orthopyroxene or amphibole) reacted together to form the symplectic intergrowth. Thus, the symplectic intergrowth occurred only where these are in direct association. The associated discrete oxide grains supplied the large amount of iron and titanium needed, and the residual melt provided the minor elements as well as served as a sink for magnesium.

REFERENCES

REFERENCES

Albee, A. L. and F. R. Ray (1970) Correction factors for electron probe microanalysis of silicates, oxides, carbonates, phosphates, and sulfates. Anal. Chem., 42, 1408-1414.

Ambler, E. P. and P. M. Ashley (1977) Vermicular orthopyroxene-magnetite symplectites from the Waterangs layered mafic intrusion, Queensland, Australia. Lithos, 10, 163-172.

Ambler, E. P. and P. M. Ashley (1980) Mineralogy and petrology of the Dutchmans Creek gabbro intrusion, South Carolina: discussion. Am. Mineral.,65, 1302-1303.

Anderson, A. T., Jr. (1966) Mineralogy of the Labrieville anorthositc, Quebec. Am. Mineral., 51, 1671-1712.

Anderson, A. T., Jr. (1968) Oxidation of the LaBlanche Lake titaniferous magnitite deposite, Quebeck. J. Geol., 76, 528-547.

Basley, J. R. and F. Buddington, (1958) Iron-titanium oxide minerals, rocks and aeromagnetic anomalies of the Adirondacks area, N.Y. Econ. Geology, 53, 777-805.

Bence, A. E. and A. L. Albee (1968) Empirical correction factors for the electron microanalysis of silicates and oxides. J. Geol., 76, 382-403.

Buddington, A. F. and D. H. Lindsley (1964) Iron-titanium oxide minerals and synthetic equivalents. J. Petrol., 5, 310-357.

Burton, B. (1984) Thermodynamic analysis of the system Fe_2O_3-$FeTiO_2$. Phys. Chem. Minerals, 11, 132-139.

Butler, J. R. and P.C. Ragland, (1969) A petrochemical survey of plectonic intrusions in the Piedmont, Southeastern Appalachians, U.S.A. Contrib. Mineral. Petrol., 24, 164-190.

Cabaup, J. (1969) Origin and differentiation of the gabbro in the Concord ring dike, North Carolina Piedmont. Unpublished M.S. Thesis, University of North Carolina at Chapel Hill.

Carmichael, C. M. (1961) The magnetic properties of ilmenite-hematite crystals. Proc. Royal Soc., 263A, 508-530.

Czamanske, G. K. and P. Mihalik (1972) Oxidation during magmatic differentiation, Finnmarka Complex, Oslo area, Norway: Part 1, the opaque oxides. J. Petrol., 13, 493-509.

Daval, D. (1987) Petrogenesis of orthopyrxene-magnetite-ilmenite intergrowths from an ultramafic layer. Contrib. Mineral. Petrol., 95, 301-310.

Duchesne, J. C. (1970) Microtextures of the Fe-Ti Oxide minerals in the South-Ragaland anorthositic complex (Norway). Ann. Soc. Geol. Belg., 93, 527-544.

Duchesne, J. C. (1972) Iron titanium oxide minerals in the Bjer Kremsogndal Massif, south-western Norway. J. Petrol., 13, 57-81.

Elsdon, R. (1971) Clinopyroxenes from the Upper Layered Series, Kap Edvard Holm, east Greenland. Mineral. Mag., 38, 49-57.

Elsdon, R. (1972 Iron-titanium oxide minerals in the Upper Layered Series, Kap Edvard Holm, east Greenland. Mineral. Mag., 38, 946-956.

Esbensen, K. H. (1978) Coronites from the Fongen gabbro complex, Trodhein region, Norway: role of water in the olivine-plagioclase reaction. Neuse Jahrb. Mineral. Abh., 132, 113-135.

Fleet, M. E., G. E. Bilcox, and R. L. Barnett (1980) Oriented magnetite and ilmenite inclusions in pyroxenes from the Grenville Province. Can. Mineral., 18, 89-99.

Foslie, S. (1928) Gleichgewichtsverhaltnisse bei einigen titaneisenerzen. Fennia, 50, 1-15.

Fullagar, P. D. (1971) Age and origin of plutonic intrusions in the Piedmont of Southeastern Appalachians. Geol. Soc. Am. Bull., 82, 2845-2862.

Garrison, J. R. and L. A. Taylor (1981) Petorgenesis of pyroxene-oxide intergrowths from kimberlite and cumulate rocks: co-precipitation or exsolution? Am. Mineral., 66, 723-740.

Goode, A. D. T. (1974) Oxidation of Natural olivines. Nature, 248, 500-501.

Gruenewaldt, G. von, D. D. Klenn, and R. M. Dehn (1985) Exsolution features in titano magnetites from massive magnetite layers and their host rocks of the upper zone, eastern Bushveld Complex. Eco. Geol., 80, 1049-1061.

Haggerty, S. E. (1976) Oxidation of opaque mineral oxides in basalts, in Rumble, D. (ed). Oxide Minerals, Chap. 4. Mineral Soc. Am. Short Course Notes 3, Hg1-100.

Haggerty, S. E. (1976) Opaque mineral oxides in terrestrial igneous rocks, in Rumble, D. (ed.). Oxide Minerals, Chap. 8. Mineral Soc. Short Course Notes 3, Hg101-300.

Haggerty, S. E. and I. Baker (1967) The alteration of olivine in basaltic and associated lavas. Contrib. Mineral. Petrol., 16, 233-257.

Hamilton, D. C., C. W. Burnham, and E. F. Osborn (1964) The solubility of water and effects of oxygen fugacity and water content on crystallization in mafic magmas. J. Petrol., 5, 21-39.

Haselton, J. D. and W. P. Nash (1975) Ilmenite orthopyroxene intergrowths from the Moon and Skaergaard intrusion. Earth Planet. Sci. Lett., 26, 287-291.

Heier, K. (1956) Thermometric and petrogenic significance of titaniferous magnetite-discussion. Am. J. Sci., 254, 506-515.

Hermes, O. D. (1968) Petrology of the Mecklenburg gabbro-metagabbro complex, North Carolina. Contrib. Mineral. Petrol., 18, 270-294.

Hermes, O. D. (1970) Petrochemistry of coexistent mafic silicates from the Mecklenburg gabbro-metagabbro complex, North Carolina. Bull. Geol. Soc. Am., 81, 137-164.

Himmelberg, G. R. and A. B. Ford (1977) Iron-titanium oxides of the Dufek intrusions Antarctica. Am. Mineral., 62, 623-633.

Kretchsmar, U. H. and R. H. McNutt (1971) A study of the Fe-Ti oxides in the Whitestone north site, Dunchrunch, Ontario. Can. J. Earth Sci., 8, 947-960.

Lamoen, H. van (1979) Coronas in olivine gabbros and iron ores from Susimak; and Riuttanaa, Finland. Contrib. Mineral. Petrol., 68, 259-268.

Lindsley, D. H. (1976) Experimental studies of oxide minerals, in Rumble, D. (ed.). Oxide Minerals, Chap. 2, Mineral Soc. Am. Short Course Notes 3, L 61-88.

Mathison, C. I. (1975) Magnetites and ilmenites in the Somerset Pan layered basic intrusion, southeastern Queensland. Lithos, 8, 93-111.

McSween, H. Y., Jr. (1980) Mineralogy and petrology of the Dutchmans Creek gabbroic intrusion, South Carolina: reply. Am. Mineral., 65, 1304-1306.

McSween, H. Y., Jr. (1986) The Concord gabbro-syenite complex, North Carolina. Geol. Soc. of Am. Cenn. Field Guide--S. E. Sec., 52, 231-233.

McSween, H. Y., Jr. and P. G. Nystrom (1979) Mineralogy and petrology of the Dutchmans Creek gabbroic intrusion, South Carolina. Am. Mineral, 64, 531-545.

McSween, H. Y., Jr., T. W. Sando, S. R. Clark, J. T. Harden, and E. A. Strange (1984) The gabbro-metagabbro association of the southern Appalachian Piedmont. Am. J. Sci., 284, 437-461.

Medlin, J. H., C. P. Thornton and D. P. Gold (1972) Petrology of mafic igneous complexes in the southeastern U.S. Piedmont: II. The Buffalo mafic igneous complex, Union County, South Carolina. Southeastern Geol., 14, 73-106.

Muir, I. D., C. E. Tilley, and J. H. Scoon (1957) Contribution to petrology of Hawaiian basalts, I. the picrite basalts of Kilawea. Am. J. Sci., 255, 241-253.

Neumann, E. R. (1974) The distribution of Mn^{2+} and Fe^{2+} between ilmenite and magnetite in igneous rocks. Am. J. Sci., 274, 1074-1088.

Olsen, B. A. (1972) Petrogenesis of the Concord gabbro-syenite complex, Cabarrus County, North Carolina. Unpublished M.S. Thesis, University of Tennessee at Knoxville.

Olsen, B. A., H. Y. McSween, and T. W. Sando, (1983) Petrogenesis of the Concord gabbro-syenite complex, North Carolina. Am. Mineral., 68, 315-333.

Osborn, E. F. (1962) Reaction series for subalkaline igneous rocks based on different oxygen pressure conditions. Am. Mineral., 47, 211-226.

Otten, M. T. (1983) The magmatic and subsolidus evolution of the artifjalletgabbro Central Swedish caledonides. Alblassendan: Offsetdrukkenij Kanters B. V.

Plas, L. van der and A. C. Tobi (1965) A chart for judging the reliability of point counting results. Am. J. Sci., 263, 87-90.

Price, G. D. (1979) Microstructures in titanomagnetites as a guide to cooling rates of a Swedish intrusion. Geol. Mag., 116, 313-318.

Ramdohr, P. (1980) The Ore Minerals and their Intergrowths. Second Edition. Oxford: Pergamon Press.

Schulze, D. J., H. Helmstaedt, and R. M. Cassie (1978) Pyroxene-ilmenite intergrowths in garnet pyroxenite zenoliths from a New York Kimberlite and Arizona latites. Am. Mineral., 63, 258-265.

Thy, P. (1982) Titanomagnetite and ilmenite in the Fongen-Hyllingen basic complex, Norway. Lithos, 15, 1-16.

Turnock, A. C. and H. P. Eugster (1962) Fe-Al oxides: Phase relationships below 1000°C. J. Petrol. 3, 533-565.

Vincent, E. A. and R. Phillips (1954) Iron-titanium oxide minerals in layered gabbros of Skaergaard intrusion, east Greenland. Geochem. Cosmochin. Acta, 6, 1-26.

Watson, T. L. and F. B. Laney (1906) The building and oramental stones of North Carolina. N. C. Geol. Survey Bull., 2, 283p.

Williams, H. and R. D. Hatcher (1982) Suspect terraines and accretionary history of the Appalachian orogen. Geol., 10, 530-536.

Wright, J. B. (1961) Solid-solution relationships in some titaniferous iron oxide ores of basic igneous rocks. Mineral. Mag., 32, 778-789.

VITA

Mary Lynn Dobson was born in Nashville, Tennessee on Janurary 2, 1953. She graduated from Harpeth Hall High School in June of 1971. The following September she entered the University of the South in Sewanee, Tennessee where she received a Bachelor's degree in Fine Arts. Following completion of her undergraduate studies, she was employed by the State of Tennessee as a naturalist at Rock Island State Park.

Mary Lynn was admitted to the University of Tennessee in the winter of 1980 as a special student and accepted into the Graduate program of Geology in the fall of 1981. This degree was awarded in the fall of 1987.